Wavepool in a Natural Lake Environment

A Design Study for the Edges of an Artificial Surf Reef in the Noorderplas, Roermond

Victor Gallardo Torres

Delft University of Technology

TU Delft

Wavepool in a Natural Lake Environment

A Design Study for the Edges of an Artificial Surf Reef in the Noorderplas, Roermond

by

Victor Gallardo Torres

Students:	Victor Gallardo Torres	4547845
Supervisors:	Matthieu de Schipper	TU Delft
	Steven Schmied	24/7Waves
	Will Sproncken	24/7Waves
Project Duration:	25 April 2022 - 1 July 2022	
Course Name:	Research Project CIE5050-09	

Cover Image: The Wave at Area X ; *picture by Area X*

TU Delft

24/7 WAVES

Preface

Before you lies the end product of the internship of Victor Gallardo Torres at 24/7Waves. 24/7Waves is a company that is researching, developing and operating scalable wavepool concepts for the leisure industry. Currently, the feasibility of a wavepool in the natural lake environment is investigated. Commissioned by 24/7Waves a design study is executed for the edges of an artificial surf reef in the Noorderplas in Roermond to prevent lake bank erosion. The conclusion and the recommendations are adressed to the team of 24/7Waves to expand their knowledge on the feasibility of a wavepool in a natural lake environment.

I would like to express my graditude to Matthieu de Schipper, Steven Schmied and Will Spronken for your supervision and guidance. Your extensive feedback and enthusiasm helped me a lot. I would like to thank the team of 24/7Waves for giving me this opportunity. It has been an inspiring period and I learned a lot. Not only did I expand my technical knowledge, it was truly valuable to experience to be introduced to entrepreneurship. I would like to thank Max Berning for his support, input and help during the fieldwork. The visualization of our GPS survey ended up beautiful. Lastly, I would like to thank my family, girlfriend and friends for their support.

Victor Gallardo Torres
The Hague, July 2022

Contents

1 Introduction

Wave surfing is a water sport in which a surfer uses a board to ride a wave towards the shore. It is done in the coastal areas around the globe. Each surf spot has its own wave quality depending on the wave climate and the type of coast. Some spots have year-round perfect waves and other surf spots only work 'when the stars are aligned.' The search for the perfect spot and conditions makes the sport unique and interesting. On the other hand, it makes the sport exclusive. Only people that are able to access surf spots during the right conditions have the chance to surf.

Wave surfing is becoming an increasingly popular sport. Therefore, the demand for year-round good quality waves increases as well. Since a few decades, the sport has found itself a new opportunity: the wavepool. In a wavepool the surfer rides a man-made wave. These artificial waves can be adjusted to ones preferences, can be generated whenever you want and are independent of natural circumstances. Various types of wavepools exist, each with their own technology. Engineers have the ambition to continuously improve technology and efficiency.

Area X is a water recreation area in the Weerd near Roermond. Area X is planning to construct a wavepool in the lake environment of the Noorderplas. To realize the wavepool, Area X has consulted 24/7Waves. 24/7Waves is a company that is researching, developing and operating scalable wavepool concepts. The project ambition is to create waves for beginner, intermediate and advanced surfers. The wavemaker should generate 150 waves per hour with a ride of 11 to 15 seconds per wave with a wave height up to 2 meters. Figure 1.1 gives an impression of the wavepool at the South shore of the Noorderplas.

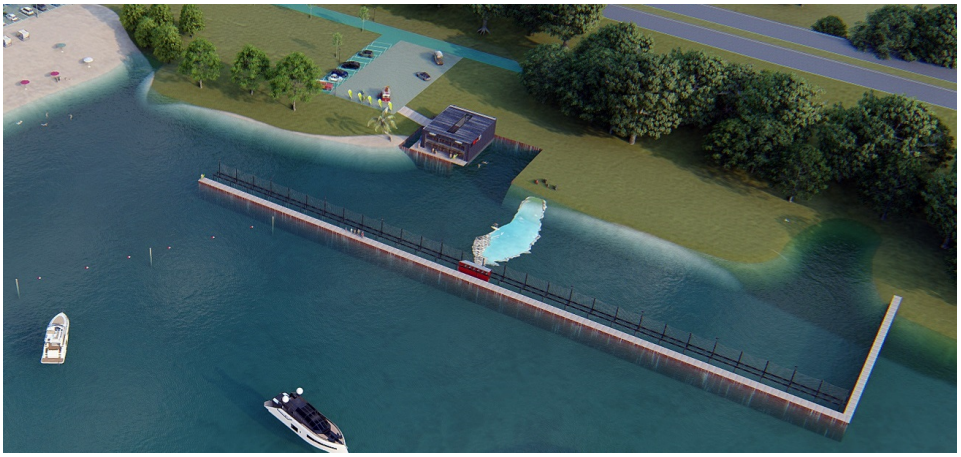

Figure 1.1: Render of the Wave at Area X ("The wave", 2020).

1.1. Problem Definition

So far, no wavepools exist in open water environments. It is unclear in what way the wavepool system and the lake system will interact. On the one hand, it is unknown what the hydrodynamic and morphodynamic impact will be from the wavepool on the lake system. Wave induced bed and bank erosion

or deteriorated water quality are for example undesired. On the other hand, it is unknown in what way the natural varying conditions of the lake system will affect the performance of the wave. Water level differences or local generated wind waves may not influence the quality of the generated wave.

Currently the first 24/7Waves full-scale wavepool prototype is being developed in the Binckhorst in The Hague. The design consists of a closed basin with a length of 150 meters long and 30 meters width and a certain bottom profile. Along the length of the basin a hull is towed back and forward in a horizontal linear path creating wave like a ship does. Figure 1.2 shows a technical drawing of the cross-section of the reef in the Binckhorst in The Hague with an artist impression of the generated wave.

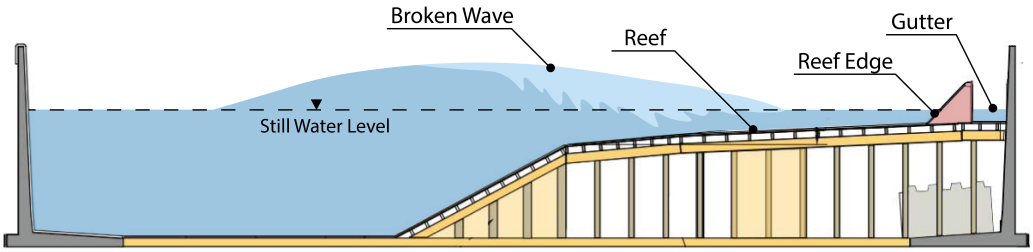

Figure 1.2: Cross-section of the wavepool in the Brinkhorst with an artist impression of the generated wave by 24/7Waves.

The design of the wavepool in the Binkhorst should be adjusted such that it can perform in harmony with the natural lake environment of the Noorderplas. Figure 1.1 gives an impression of the generated wave that propagates along the natural lake banks of the Noorderplas. Lake bed and banks that are subject to frequent wave impact are likely to erode (Duró et al., 2020). The most important element of the wavepool to prevent lake bed and bank erosion is the edge of the reef and the gutter (see Figure 1.2). The reef edge eliminates the wave from the wavepool basin and the gutter facilitates the discharge of the water that is washed over the edge.

1.2. Objective

The objective of this study is to design the edge and the gutter of the Area X wavepool in the Noorderplas to prevent lake bed and bank erosion. Further design requirements of the edge and the gutter are listed below:

- The edge should be able to dissipate a broken up to 150 mm without reflection.
- Waves originate from both spilling as plunging breakers.
- Varying lake water levels should be taken into account.
- The edge should be aesthetically pleasing.
- The existing design for the reef and the wave maker should be taken as boundary condition.

The final deliverable will be a qualitative design for the edge and the gutter of the reef. An elaboration will be given on the important design parameters to prevent wave reflection and lake bank erosion. Next to that, a first order estimate for the dimensions and possible construction materials will be given.

1.3. Methodology

First, a literature study will be carried out to form the theoretical framework for the design study. The most important phenomenon to take into consideration for the design will be sorted out. The topics that will be sorted out in the literature study are listed below:

- Wave hydrodynamics
- Ship waves and Loads on bed and banks
- Wave attenuation methods
- Wavepool technology

After that an area study will be executed. In the area study the natural boundary conditions for the design will be sorted out. The important aspects, such as the hydrodynamic conditions, bathymetry and sediment characteristics of the Noorderplas will be analysed. A field survey will be executed to get acquainted with the locations. Depending on the already available data, the following surveys are proposed: a bathymetry and topography survey to map the lake bed and ground profiles of the project location and an inspection of the lake bed sediment.

In the design phase three alternatives for the edge of the reef will be designed, varying either in 3 dimensional shape or construction material. It is expected that the design strategy will start with the 24/7Waves initial edge design. With basic hand calculations the performance of the initial edge will be assessed on different phenomena (wave reflection, sediment up-stirring, current intensification and other yet to be determined phenomena). After this an iterative process starts in which a new proposed design is assessed on the same phenomena as the previous design. It is intended that in each iteration the design improves.

In the conclusion the an elaboration on the qualitative design is given. Recommendations are given for the next phases of the project and knowledge gaps are identified for future research.

Figure 1.3 shows a visualization of the methodology.

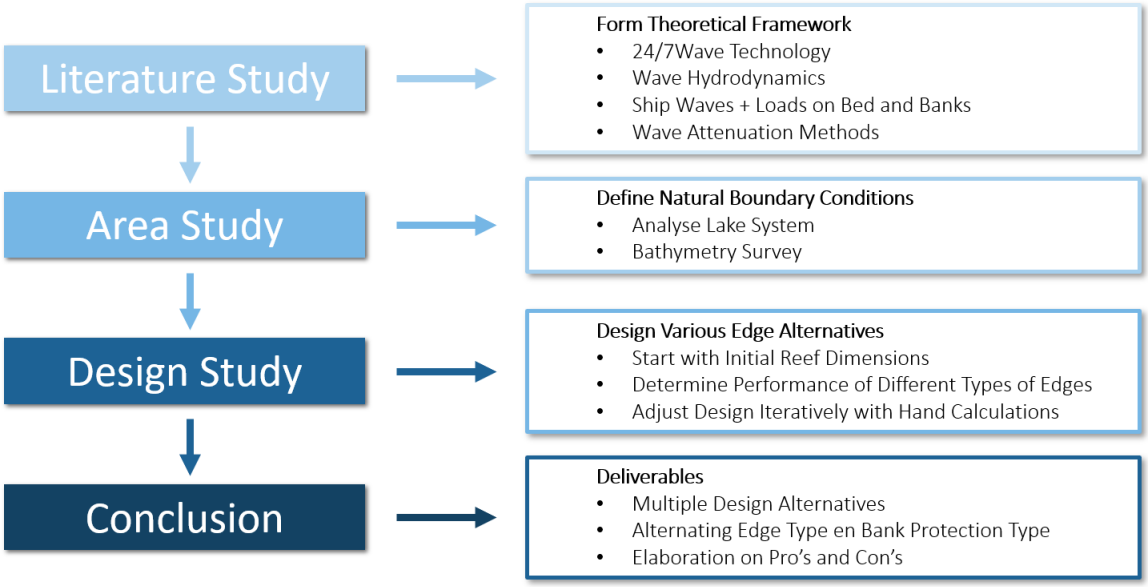

Figure 1.3: Visualization of the methodology.

1.4. Report Structure

The report is structured according to the visualization of the methodology of Figure 1.3. In chapter 2 the literature study is reported. In chapter 3 the area study is reported. In chapter 4 the design study is reported. In chapter 5 the conclusion is reported.

2

Background study

2.1. Waves

2.1.1. Introduction to waves

A water wave is defined as an oscillation of the water surface. Waves can be generated in various manners. In open water for example, short waves are usually generated by wind or by disturbances. In the ocean much longer waves are present. For example, tidal waves that are generated by attractive forces of the sun and moon on the water bodies. Schematically an oscillation of the water surface can be described with a sine or cosine function as shown in Figure 2.1. Various wave components can be distinguished. The wave crest and the wave trough, the vertical distance between the wave crest and the wave the wave height H, the amplitude a, the temporal water level elevation η, the wave length L and the wave celerity c.

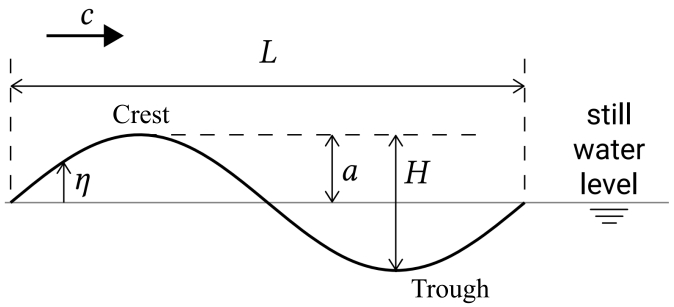

Figure 2.1: Simple representation of a wave (Bosboom & Stive, 2021).

The wave period T is the time the wave needs to pass the location and is given by $\frac{L}{c}$. The inverse of the period is the wave frequency f which describes the number of waves passing a fixed location per unit time. The surface level elevation η can be described by:

$$\eta = asin(\omega t - kx) \tag{2.1}$$

In which the angular frequency ω is given by $\frac{2\pi}{T}$ and the wavenumber k is given by $\frac{2\pi}{L}$.

Looking at any arbitrary free water surface it usually looks chaotic and irregular. In theory this irregular wave field is approximated by the random-phase/amplitude model (Holthuijsen, 2010). This is a result of the sum of a large number of harmonic waves, each with a different period, direction, amplitudes and phases. The random-phase/amplitude model is shown in Figure E.1.

The Random-phase/amplitude model is considered to be a too detailed approximation for a solitary artificial wave. In deep water, a single wave can be approximated linearly. For this case wave propagation is a matter of movement of the wave form. No actual water mass is displaced. When a wave passes, water particles namely have an orbital motion. On average their position is more or less the stationary (Bosboom & Stive, 2021). Water particles on the water surface have larger orbits than water

particles deeper in the water column. The orbital motion of a water particle due to a propagating wave is illustrated in Figure 2.2.

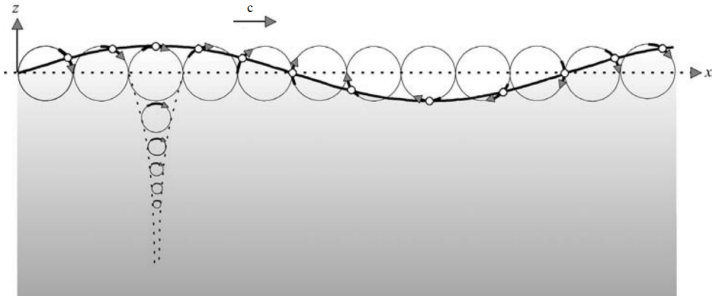

Figure 2.2: Orbital motion of water particles (Holthuijsen, 2010).

Using the continuity equation, the Navier-Stokes equations of motion and neglecting non-linearities, wave motion can be described. Neglecting non-linearities is valid for not too steep waves in deep water $(ak << 1)$ and small amplitude waves in shallow water $(a << h)$. Airy derived the so called dispersion relation which gives the relation between the frequency ω, the wavenumber k and the local water depth h. It is given by:

$$\omega = \sqrt{g \cdot k \cdot tanh(kh)} \tag{2.2}$$

The Airy wave theory gives several relations for waves depending on the local water depth as shown in Figure E.2. An other important parameter is the wave energy content per square meter of water surface E given by:

$$E = \frac{1}{8}\rho g H^2 \tag{2.3}$$

In which ρ is the density of water, g is the gravitational acceleration and H is the height of the single wave.

2.1.2. Waves in shallow water

When waves propagate from deep water into shallow water they transform. In this transformation a few important processes can be distinguished: shoaling, refraction and eventually wave breaking. At the coast these processes can be visually observed. In Figure 2.3a wave shoaling is shown, in Figure 2.3b wave refraction is shown. The white turbulent water in both pictures is the process of wave breaking.

(a) Shoaling ("Pinterest - Tamarindo C.R.", 2018)

(b) Refraction (SurferToday.com, n.d.)

Figure 2.3: Nearshore wave transformation.

Using the principle of energy conservation, offshore wave conditions can be translated to nearshore wave conditions. The following relation holds:

$$\frac{\partial}{\partial x}(Ec_g cos\theta) + \frac{\partial}{\partial y}(Ec_g sin\theta) = D \tag{2.4}$$

In this equation the first two terms represent the gradient of energy in x-direction and y-direction. θ is the wave direction with respect to the shore normal and D is the wave energy dissipation. Depth induced wave energy dissipation is generally because of bottom friction or wave breaking (Bosboom & Stive, 2021).

Shoaling
Consider a wave train that propagates from deep water towards the shore. A wave train is a group of consecutive waves with equal or similar wave lengths that propagate in the same direction. When the water depth becomes about half of the offshore wavelength L_0, the first wave in the wave train gets affected by the bottom. This will decelerate the wave. Consecutive waves that are not decelerated yet, will catch up with the first wave. This will decrease the distance between consecutive wave crest and thus decrease wavelength. It will also increase the wave height and concentrate the wave energy around the crests. Next to that, the wave orbital motions tend to become more asymmetric. The process of shoaling is schematically shown in Figure 2.4.

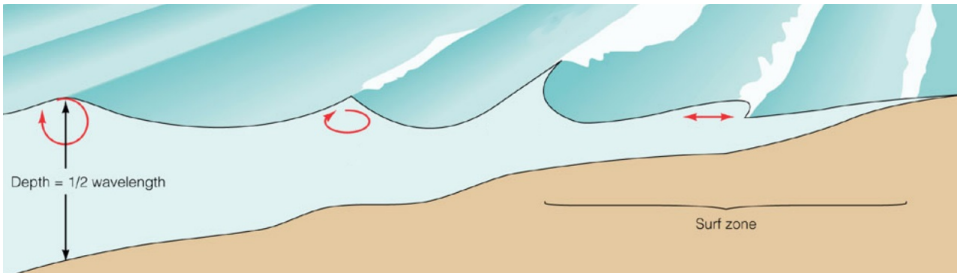

Figure 2.4: Cross-section of the nearshore beach profile. Wave shoaling happens outside the surf zone and wave breaking happens inside the surf zone (of Washington, 2006).

During the shoaling process, outside of the breaker zone, the dissipation of wave energy is approximately zero. Therefore, the energy flux U is constant during shoaling. The following relationship holds between the deep water wave height H_0 and the wave height at a certain water depth during shoaling. The shoaling factor K_{sh} describes the change in wave height during shoaling.

$$K_{sh} = \sqrt{\frac{1}{tanh(kh) \cdot 2n}} \tag{2.5}$$

In which n is the ratio between the wave group and the phase velocity.

Refraction
An other important phenomena of waves that propagate into shallow water is refraction. This is the process in which a wave crest bends towards a depth contour. When a wave approaches an alongshore uniform beach under an angle, the first section of the wave that reaches shallow water gets decelerated. This is schematically shown in Figure 2.5. The rest of the wave is still in deep water, still has its initial propagation speed and therefore moves faster than the decelerated section of the wave. The wave energy is redistributed along the wave crest and make the wave ray turn orthogonal with respect to the depth contours of the shore.

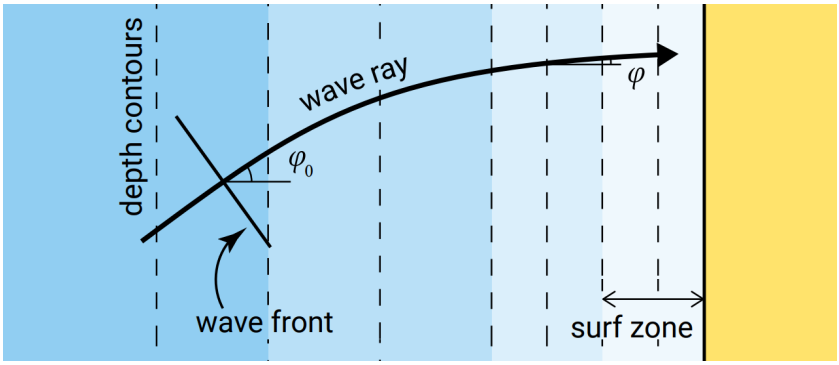

Figure 2.5: Top view of the nearshore beach profile. A wave front approaches the shore obliquely incident and turns parallel with respect to the shoreline orientation due to refraction (Bosboom & Stive, 2021).

To describe refraction Snell's law can be used. It says that

$$K_r = \sqrt{\frac{cos\phi_0}{cos\phi}} \tag{2.6}$$

In which $cos\phi_0$ is the offshore incoming wave angle and $cos\phi$ is the local wave angle.

At any location in the nearshore, before wave breaking, the wave height H can be related to the deep water wave height multiplied by the shoaling and the refraction factor.

$$H = H_0 \cdot K_{sh} \cdot K_r = H_0 \sqrt{\frac{1 \cdot c_0 \cdot b_0}{2n \cdot c \cdot b}} \tag{2.7}$$

In which H_0 is the offshore incoming wave height.

Wave breaking and breaker types
When the wave height becomes too large with respect to the wavelength a wave crest becomes unstable and the wave starts breaking. The ratio between the wave height over the wavelength is also called the wave steepness. Wave crests become unstable if the crest angle reaches about 120°. A schematic representation of this maximum crest angle is given in figure Figure 2.6

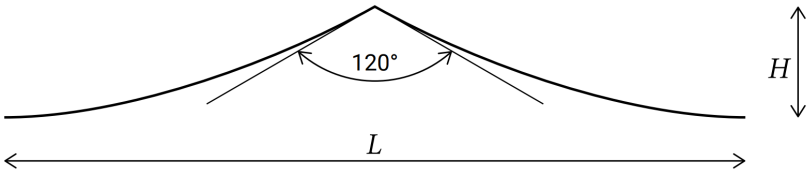

Figure 2.6: Schematic representation of wave steepness: H/L(Bosboom & Stive, 2021)

Miche has derived an expression for the limiting wave steepness based on Stokes wave theory. For shallow water the breaker index γ was derived, which shows that a single wave starts to break when the wave height becomes larger than a certain fraction of the water depth. The breaker index is shown in Equation 2.8 in which H_b is the wave height at breaking and h_b is the water depth at which the wave breaks.

$$\gamma = \frac{H_b}{h_b} \approx 0.78 \tag{2.8}$$

Depending on the wave steepness and the slope of the bed, waves tend to break differently. The Iribarren parameter ξ gives the ratio between the slope of the bed and the steepness of the wave. It is shown in Equation 2.9.

$$\xi = \frac{tan\alpha}{\sqrt{\frac{H}{L}}} \tag{2.9}$$

Battjes has related the Iribarren parameter to different types of breakers. In Figure 2.7 a schematic representation of the different breaker types is given with their typical values for the Iribarren parameter.

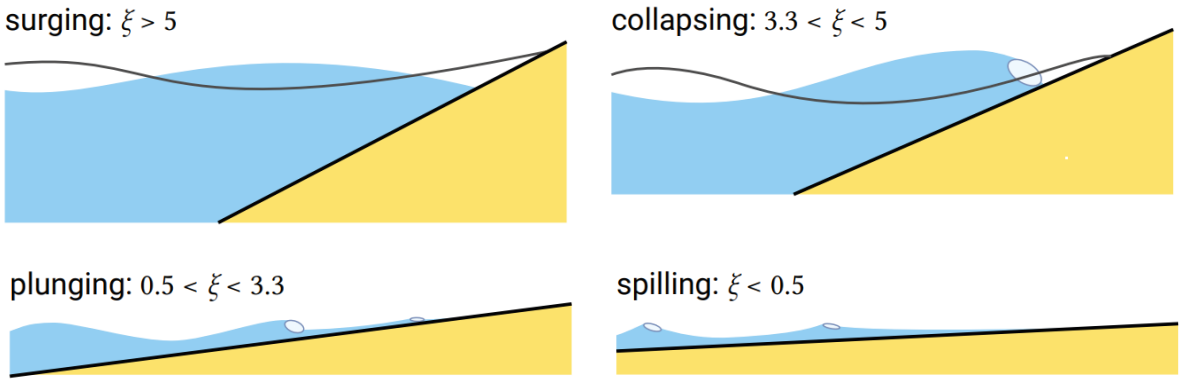

Figure 2.7: Breaker types with their Iribarren number (Bosboom & Stive, 2021)

For a Iribarren parameter of ξ < 0.5 a wave breaks spilling. When the symmetric crest of these breakers becomes in stable, it crumbles of relatively calmly. A white front, also called a surface roller, propagates towards shore over a long distance. The breaking process of a spilling breaker has usually a length of about 6 to 7 wavelengths in which almost all wave energy is dissipated (Bosboom & Stive, 2021). Little wave energy is reflected back into the water. These breakers are usually found at flat shores and are usually less challenging for surfers.

For a Iribarren parameter of 0.5 < ξ < 3.3 a wave breaks plunging. These waves are characterized by a strongly asymmetric crest that curls over and encloses an pocket of air. When the crest collapses, a water jet has a power full impact on the leading slope of the wave. The length of the breaking process is shorter than for a spilling breaker. For plunging breakers a lot of wave energy is dissipated into turbulence. Wave energy is both reflected back to the sea and transmitted towards the coast. These waves are considered to be more challenging for surfers.

Steeper shores with long swell waves are characterized by breakers that behave almost like a standing wave. Wave surges up and down the slope and the crest barely tumbles over the toe.These surging or collapsing breakers typically have an Iribarren parameter of ξ > 3.3 and are considered unsurfable (Schmied, 2014).

The water depth at which a wave breaks depends also on the bottom slope. At steeper slopes waves break at smaller water depths and at milder slopes waves break at larger water depths. Experiments have shown that the quantitative relation between the Iribarren number ξ and the breaker index γ are as shown in Table 2.1.

Table 2.1: Typical values for spilling and plunging breakers

Breaker type	Iribarren parameter	Breaker index
Spilling	ξ < 0.5	0.6 < γ < 0.8
Plunging	0.5 < ξ < 3.3	0.8 < γ < 1.2

After breaking, the wave behaves like a moving hydraulic jump or like a bore. The wave height remains equal to a fixed fraction of the local water depth $H = \gamma \dot{h}$, with constant γ.

These so called, surface rollers are a turbulent mixture of water and air that propagate towards the shore in the upper part of the water column with a speed of $c = \sqrt{gh}$. Wave energy is converted into turbulent kinetic energy and eventually dissipates. Depending on the type of breaker the wave energy

dissipates over a certain distance. The energy dissipation of a plunging breaker is concentrated around the break point. The energy dissipation of a spilling breaker is more spread out over the bottom slope. This can be seen in the schematic representation of wave energy dissipation in Figure 2.8.

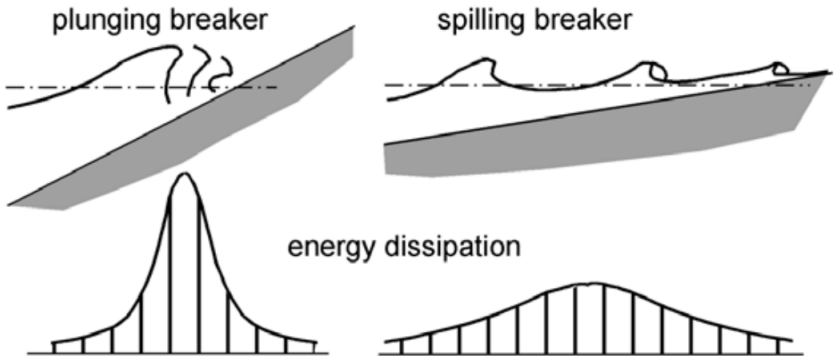

Figure 2.8: Wave energy dissipation during breaking (Schiereck, 2017)

Schiereck, 2017 mentions that the total energy loss in a bore can be approximately computed using the analogy of a hydraulic jump with:

$$D_w = \rho g \frac{H^3}{4Th} \tag{2.10}$$

Wave induced currents
After breaking, the wave induced momentum or mass transport is substantial. In the surf zone wave induced momentum per unit surface area in wave propagating direction can be described by the sum of wave energy of breaking and non-breaking waves over their velocity as indicated in Equation 2.11. For solitary breaking waves, such as a single generated wave in the wavepool, it is assumed the momentum is described by only the non-breaking term or the breaking term.

$$q_{drift} = q_{non-breaking} + q_{breaking} = \frac{E}{c} + \frac{E_r}{c} \tag{2.11}$$

In which E is the wave energy and E_r is the roller energy, c is the wave celerity and α is a factor ranging from 0.22 to 2. It should be noted that the wave induced currents only take place in the top of the water column from the wave through up to the wave crest. When a normally incident broken wave approaches a closed boundary such as an alongshore, continuity states zero net mass transport through the vertical needs to be zero, hence a return current at the bottom of the water column. The wave induced current profile over the vertical is shown in Figure 2.9

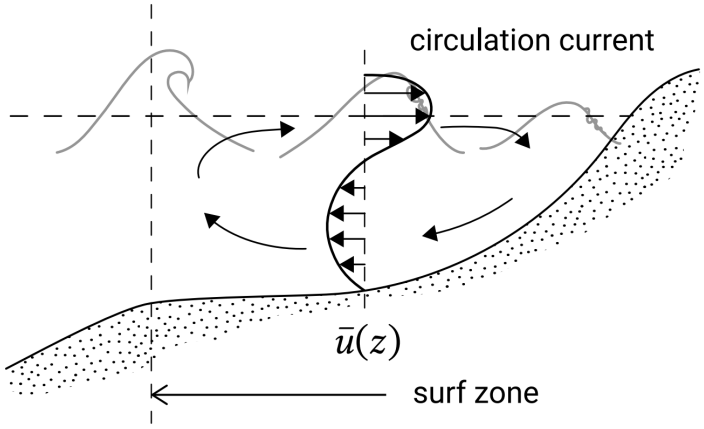

Figure 2.9: Wave induced current profile over the vertical (Bosboom & Stive, 2021).

On top of this, a normally incident broken wave that approaches an alongshore uniform coast gives rise to a water level set-up at the shore. When a wave approaches shallow water it decelerates. The deceleration causes a gradient in wave momentum transfer and a force in landward direction. This wave force is balanced with a water level gradient in the cross-shore called wave induced set-up. For obliquely incident waves that approach an infinitely long uninterrupted alongshore uniform coast no hydraulic pressure gradient can develop. Equilibrium in forces is restored by bed shear stresses developed when a longshore current is present. Holthuijsen, 2010 approximates the depth-averaged longshore current by the force balance between the gradient in wave momentum transfer and the bed friction force. With this approximation, the depth-averaged longshore current at location x in the surf zone is given by:

$$V(x) = -\frac{5}{16}\pi\frac{\gamma}{cf}\frac{sin\phi_0}{c_0}\frac{dh}{dx} \tag{2.12}$$

In which γ is the breaker parameter that is kept constant, ϕ_0 is the offshore incoming wave angle, c_0 is the deep water wave celerity, h is the local water depth, $\frac{dh}{dx}$ is the local gradient of the beachslope and cf is the dimensionless bottom friction factor. With Equation 2.12 the cross-shore distribution of the depth-averaged longshore current is computed and shown in the left panel of Figure 2.10. The figure indicates the order of magnitude of the depth-averaged longshore current for the following input parameters: $H_0 = 2m$, $\phi_0 = 30°$, γ = 0.8, a bottom slope of 1:100 and $T = 7s$. At the break point, V has its maximum and gradually dissipates land inward. The right panel of Figure 2.10 shows a top view of an obliquely incident irregular wave field approaching a longshore uniform coast. The cross-shore distribution of the depth-averaged longshore wave induced current for a more irregular wave field is indicated.

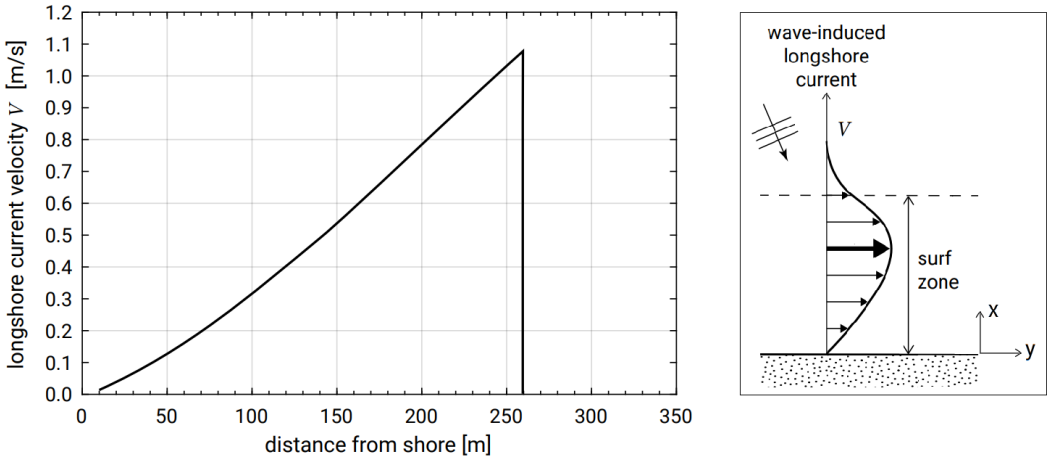

Figure 2.10: Left: computed cross-shore distribution of the depth-averaged longshore current for $H_0 = 2m$, $\phi_0 = 30°$, γ = 0.8, a bottom slope of 1:100 and $T = 7s$. Right: cross-shore distribution of the depth-averaged longshore wave induced current for a more irregular wave field (Bosboom & Stive, 2021).

2.1.3. Ship waves

When a ship sails through a channel, it creates complex wave patterns and currents. These ship waves and currents can have significant impact on the banks and the bed of navigation channels. In Figure 2.11 the wave pattern behind a ship and the erosion of the bank can be seen. The hydrodynamic processes caused by a sailing ship can be divided into two components: the primary and the secondary ship wave. The primary ship wave is a result of water pushed to the front, aside and downwards, creating a return current under the ship. Because of this return current, around the hull of the ship a water level depression can be observed. This V-pattern that can be observed behind a moving ship is called the secondary wave and is a result of a moving point disturbance in water. The primary and secondary waves have different characteristics and thus different impact on the surroundings (van Koningsveld & de Vriend, 2021). Both primary and secondary waves behave like normal water waves

(Schiereck, 2017). The propeller of the ship also has a significant impact on the surroundings. As the 24/7Waves wave making technology does not include a propeller, it is left out consideration.

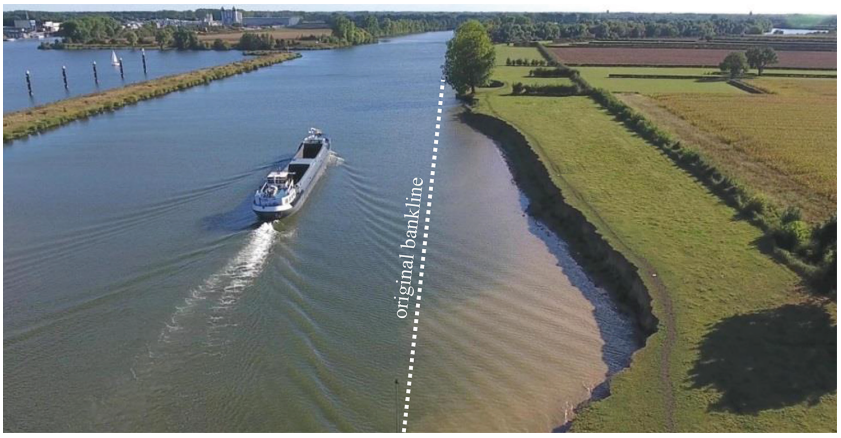

Figure 2.11: Wave pattern behind a ship and bank erosion at a reach of the Meuse river (Duró et al., 2020).

In Figure 2.12 the water level elevations after a ship passage is shown. In panel a the water level depression can be seen. The terrace at the foot of the upper bank emerges. In panel b it can be seen that due to the secondary waves a current towards the bank prevails and waves break on the foot of the upper bank. In panel c the water level elevation signal during the ships passage is shown. The elevation is zero before the ship passes. The elevation drops with the water level depression due to the primary wave. The smaller oscillations are the secondary waves that pass by.

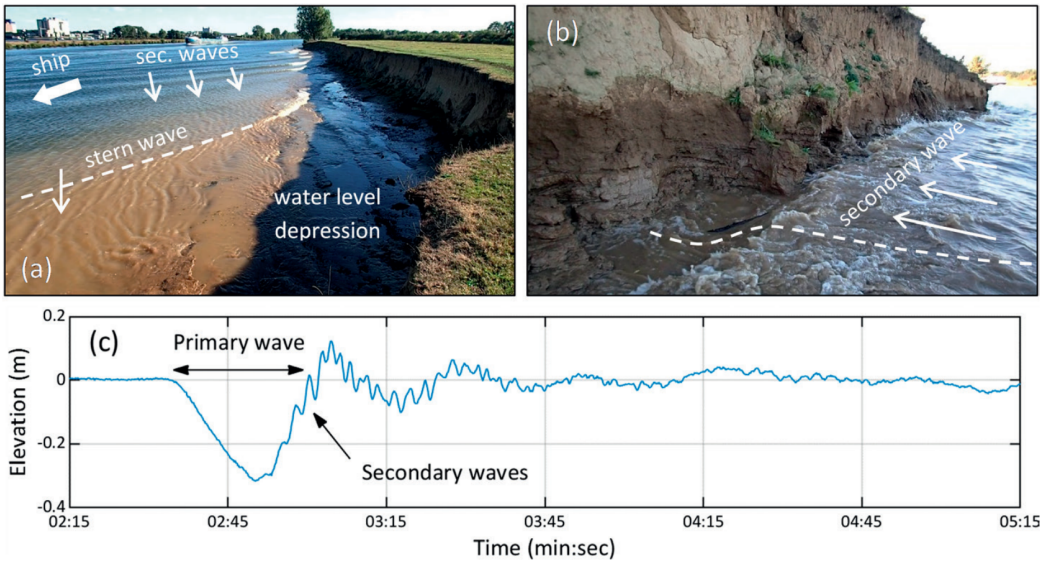

Figure 2.12: "(a) Primary and secondary waves after a ship passing. (b) Secondary wave impacting a bank with signatures of erosion and undermining. (c) Example of water level fluctuations with respect to river stage due to a passing ship."(Duró et al., 2020)

An important parameter to introduce is the Froude depth number Fr_h. According to Schijf, the Froude depth number can be used to assess whether deep or shallow water conditions hold for a sailing ship. For slower sailing speeds or deeper water the Froude depth number can become smaller than 0.74 which indicates a subcritical return current and the ship experiences deep water conditions. The return current becomes critical, the Froude depth number becomes 1. For larger Froude depth numbers the return current becomes supercritical. The Froude depth number is given by the proportion between the sailing speed and the shallow water wave celerity:

$$Fr_h = \frac{V_s}{\sqrt{gh_0}} \tag{2.13}$$

Primary ship waves

The primary ship wave has the characteristics of a negative solitary wave and has a four main components: the front wave, with a height z_{front}, a water-level depression z around the ships hull, a return current u_r and the stern wave, with a height of z_{max}. Figure 2.13 shows a cross and side view of a ship navigating in a channel. The components of the primary ship wave are indicated in the figure.

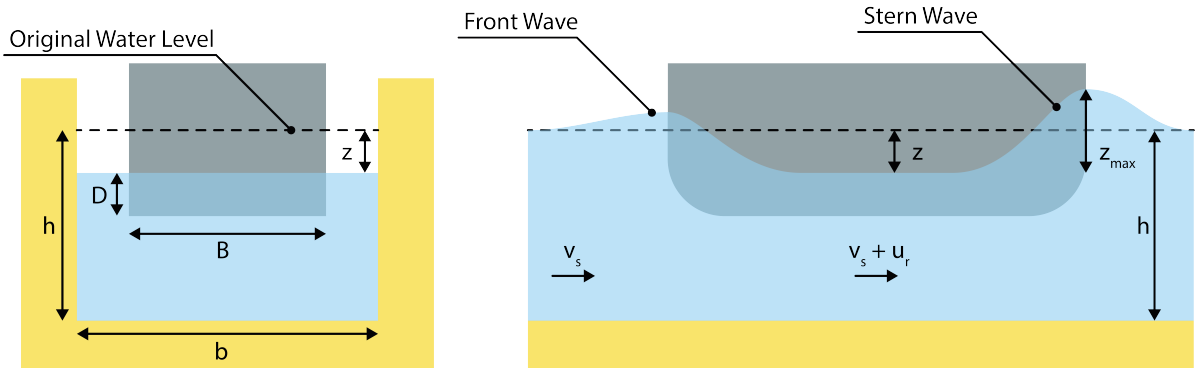

Figure 2.13: Cross view and side view of a ship in a channel. Indicated are the primary wave components to form the basis of the 1-D approach.

When the cross-section area of the ship A_s is considerable with respect to the cross-section area of the channel A_c, the hydrodynamics around the ship can be schematized as a 1-D flow situation. Schijf has done this considering the ship to be stationary and the water flows with v_s. From Bernoulli and continuity the water-level depression z and the return current u_r can be derived. Assuming among others a constant water-level depression and return flow over the channel's cross-section. This approach is only valid if the width of the ship W_s is smaller than 1.5 times the length of the ship L_s ($\frac{W_s}{L_s}$ < 1.5) (van Koningsveld & de Vriend, 2021). Schiereck, 2017 approximates the height of the stern wave z_{max} as in Equation 2.16.

$$\frac{v_s^2}{gh} = \frac{2z/h}{(1 - A_s/A_c - z/h)^{-2} - 1} \tag{2.14}$$

$$\frac{u_r}{\sqrt{gh}} = \left(\frac{1}{1 - A_s/A_c - z/h} - 1\right) \frac{v_s}{\sqrt{gh}} \tag{2.15}$$

$$z_{max} = 1.5 \cdot z \tag{2.16}$$

Secondary ship waves

Secondary ship waves behave like a number of consecutive periodic waves also called a wave train. They are caused by the pressure pattern due to discontinuities of the ships hull. These discontinuities are located at the bow and the stern of the ship of which the bow is usually dominant. While sailing, each disturbance of the ship creates a circular wave. The remains of these circular waves are called the transverse waves and propagate in the same direction and with the same speed as the ship. A diverging wave envelops the path of circular waves. The location where transverse and diverging waves meet, interference cusps or featherlet waves are formed. The transverse, diverging and cusps are illustrated in Figure 2.14. Featherlet waves are dominant for the stability of revetments (Schiereck, 2017).

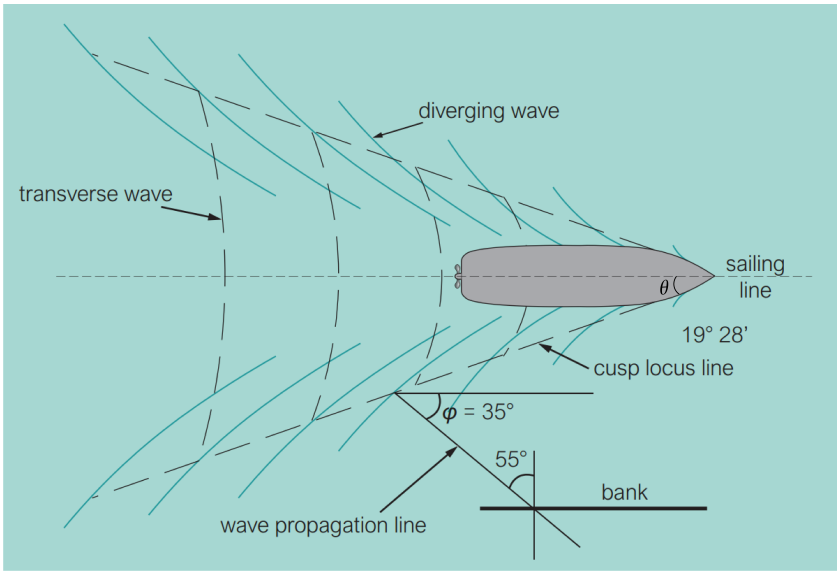

Figure 2.14: Deep water secondary wave pattern from the bow (van Koningsveld & de Vriend, 2021)

The height of the cusps is a summation of the heights of both incoming waves. Verheij and Bogaerts derived empirically the following relation for the maximum height of the interference cusps for Froude depth numbers smaller than 0.8.

$$H_i = 1.2 \cdot \alpha_i \cdot h_0 \cdot (\frac{y_s}{h_0})^{-0.33} \cdot Fr_h^4 \tag{2.17}$$

This relation is only valid if $h_0/L_{cusps} > 0.25$, $H_i/L_{cusps} < 0.14$ and $H_i/h_0 < 0.6$. Next to that, (van Koningsveld & de Vriend, 2021) gives some relations for the propagation speed and the wave length of the cusps.

$$c_{cusp} = V_s cos\phi \tag{2.18}$$

$$L_{cusp} = 4.2 \cdot h_0 \cdot Fr_h^2 \tag{2.19}$$

For moderate sailing speeds, cusps propagate under an angle of ϕ = 35° with respect to the sailing speed. For larger sailing speeds eatherlet waves propagate more in the direction of sailing. The direction of cusp propagation can also be expressed with the angle of the cusp locus line θ. The graph in Figure 2.15 shows the relation between the Froude depth number and the angle of the cusp locus line θ.

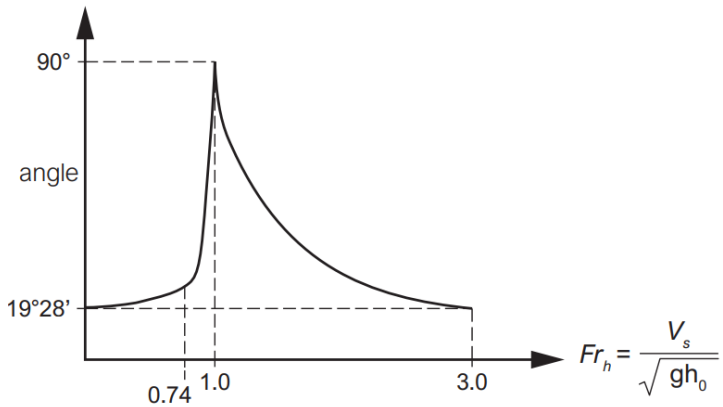

Figure 2.15: Angle of the cusp locus line θ and the Froude depth number (van Koningsveld & de Vriend, 2021)

2.1.4. Wave induced sediment transport

Initiation of sediment particle motion

A sediment particle can be transported by water. A single sediment grain is set in motion if the water movement exerts a large enough shear stress. The forces that act on a single sediment grain are shown in Figure 2.16. Analysing these forces (drag force, lift force and gravity) a critical condition can be found for the initiation of motion of the single grain.

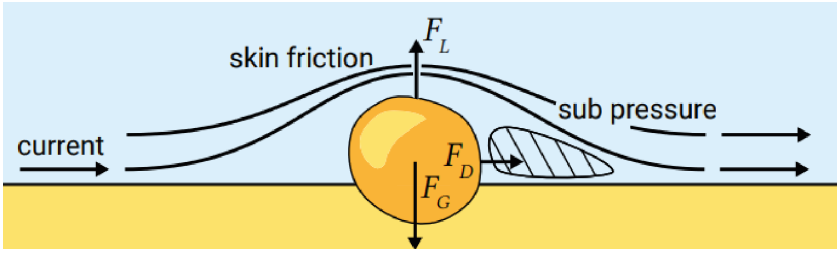

Figure 2.16: Forces on a single sediment grain. Drag force by skin friction, lift force by flow separation and contraction and the restoring gravity force (Bosboom & Stive, 2021).

With this starting point Shields derived a relation (Equation 2.20) between the driving forces and the resisting forces for the initiation of motion. The so called critical shields parameter θ_{cr} indicates whether a particle is set in motion by a current.

$$\theta_{cr} = \frac{\tau_{b,cr}}{(\rho_s - \rho)gD} \tag{2.20}$$

The shear stress that initiates particle motion is called the critical shear stress $\tau_{b,cr}$ and is a function of the horizontal current velocity and a bed friction factor cf. The horizontal current velocity for waves varies over the wave motion. Therefore, the critical bed shear stress induced by waves is a function of the amplitude of the waves orbital motion near the bed. The relation is shown in Equation 2.21.

$$\tau_b = \rho_w \cdot cf \cdot u_0^2 = \rho_w \cdot cf \cdot \frac{\omega H}{2sinh(kh)} \tag{2.21}$$

Types of sediment transport

For different values of the Shields parameter different types of sediment transport can be distinguished. The types of sediment transport are shown in Figure 2.17.

- Bed load transport: this is rolling type of sediment transport in a thin layer close to the bed. Particles are in constant contact with the bed. Typical values for the Shields parameter are between 0.03 and 0.06.
- Sheet-flow transport: this is rolling and jumping type of sediment transport in a larger layer close to the bed. Typical values for the Shields parameter are between 0.8 and 1.
- Suspended load transport: this is the transport of particles that are suspended and don't make any contact with the bed. Typical values for the Shields parameter are larger than 1.

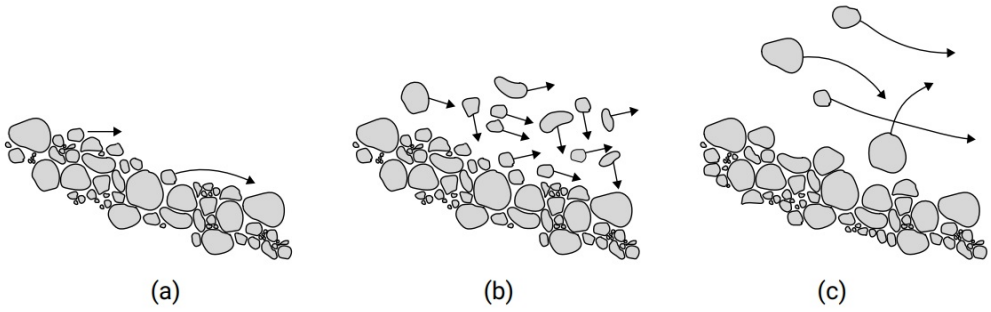

Figure 2.17: A: Bed load transport. B: Sheet-flow transport. C: Suspended load transport (Bosboom & Stive, 2021).

An example for a formulation of sediment bed load transport is given by:

$$S_b = BD_{50} \cdot \frac{U\sqrt{g}}{C} \cdot exp(\frac{-0.27(s-1)D_{50}\rho g}{\mu \cdot < |\tau_{cw}| >}) \tag{2.22}$$

There will not be elaborated on each different parameters influencing the bed load transport. The most important thing that should be noted is that a formulation for the bed load transport knows a current related term and a wave induced shear stress related term. Bosboom and Stive, 2021 mention that: ”waves stir up the sediment, while currents transport it.”

Longshore sediment transport continuity
A method to estimate the bulk longshore sediment transport over the breaker zone as a function of the angle of incidence of incoming waves is the CERC formula. The CERC formula is widely used despite the fact that the physical processes are strongly simplified. Only the effect of wave induced alongshore current is considered, other currents such as tidal currents are neglected. Next to that, the CERC formula neglects sediment properties such as grain size. The sediment transport is averaged over the cross-shore direction in the breaker zone. For an offshore wave height of H_0 = 2 m and a wave period of T = 7 s, the bulk longshore sediment transport can be plotted as a function of the offshore incoming wave angle as follows, seen in Figure 2.18. It can be seen that for normal incident waves, with a offshore incoming wave angle of ϕ_0 = 0°, the longshore sediment transport equals 0. For absolute increasing wave angles the transport rates also increase in absolute sense. The maximal absolute longshore sediment transport is found at an offshore incoming wave angle of $\phi_0 \approx 43°$.

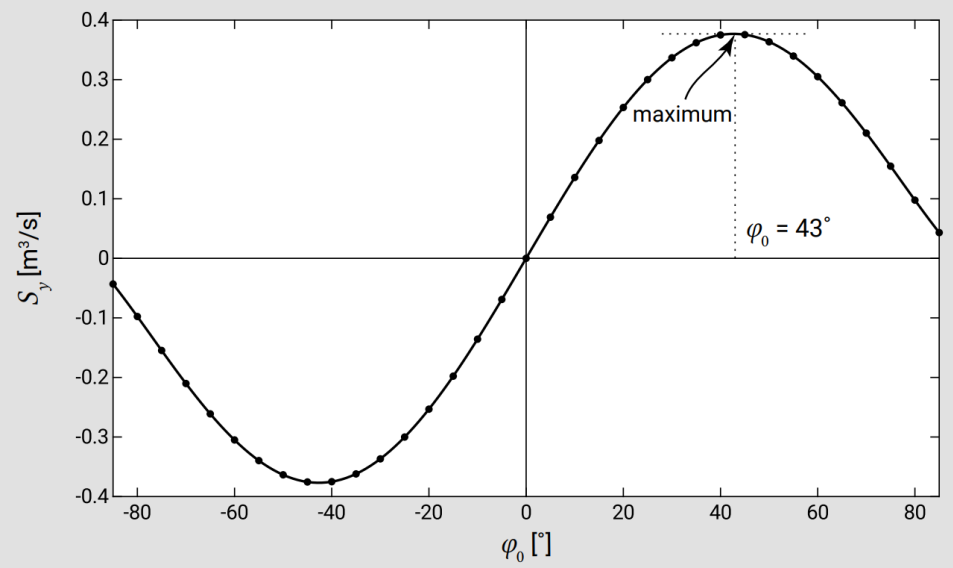

Figure 2.18: ”Bulk longshore transport rates S as a function of the deep water wave angle ϕ_0” (Bosboom & Stive, 2021).

In Figure 2.19 a schematic top view of a coastline is shown. The development of a section of the coastline can be analysed if the sediment fluxes at the boundaries of the section are defined as S_{in} and S_{out}. The section of the coastline will remain stable in time as long as the incoming sediment volume equals the outgoing sediment volume: $S_{in} = S_{out}$. The section of the coastline will move land inward if the outgoing sediment volume is larger than the incoming sediment volume: $S_{out} > S_{in}$. Figure 2.19 shows the beach line at $t = 0$ and the retreated coastline at $t > 0$ for $S_{out} > S_{in}$.

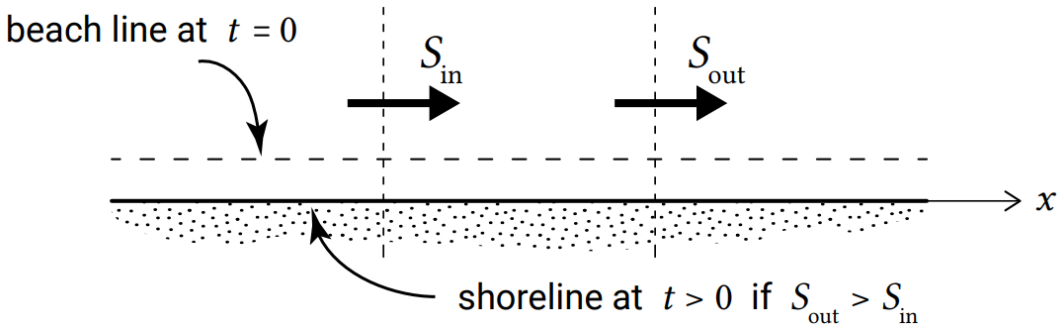

Figure 2.19: Top view of a coastline with the coastline development schematically indicated (Bosboom & Stive, 2021).

2.1.5. Wave load reduction

Several measures can be taken to reduce wave loads that reach the coast. When waves propagate over slopes or wave reducing devices (such as breakwaters or vegetation), wave energy gets reflected, transmitted or absorbed. Schiereck, 2017 mentions that the best wave reductor is probably a shallow and mildly sloping foreshore. Here waves can brake gradually over a larger distance and the wave load is spread out by bottom friction.

A method to describe the damping effect of structures on waves is with the transmission coefficient K_T (d'Angremond et al., 1997). K_T gives the ratio between the transmitted wave height H_T and the incoming wave height H_I. K_T describes the fraction of the incoming wave energy that is found downstream of a slope or wave load reduction device.

$$K_T = \frac{H_T}{H_I} \tag{2.23}$$

Wave energy that is not transmitted is reflected or absorbed. Wave reflection can be described by the reflection coefficient K_R. The reflection coefficient is given by the ratio between the reflected wave height H_R and the incoming wave height H_I.

$$K_R = \frac{H_R}{H_I} \tag{2.24}$$

Battjes, 1974 has found an exponential relation between K_r and the Iribarren parameter ξ. For $\xi > 2.5$, K_R slowly reaches full reflection. The relation can be seen in Figure 2.20.

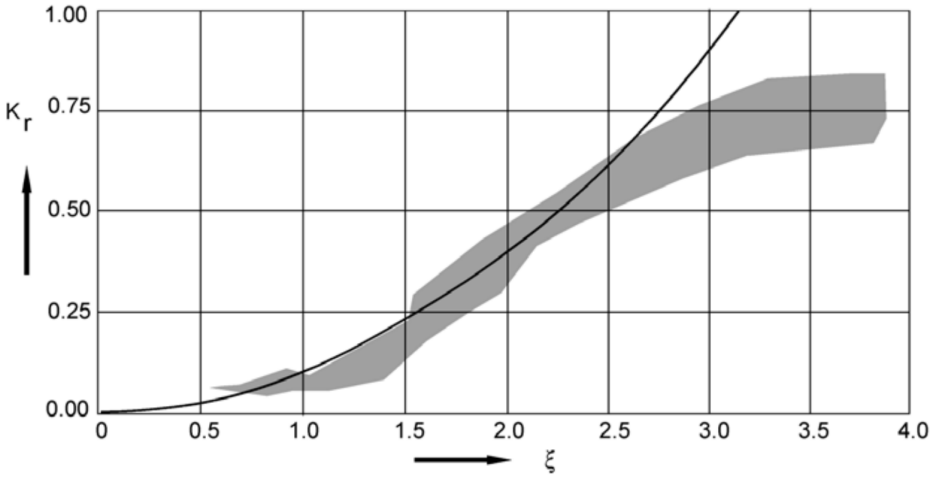

Figure 2.20: Wave reflection as a function of the Iribarren number ζ (Battjes, 1974).

Wave energy absorption happens when the water in the waves flows through constructive parts of the wave reduction device such as stones or roots. The waves that run over and flow through the device can result in internal work or movement of the device. Absorption of wave energy is at the expense of the bed and bank protection layer or the wave load reduction structure. Schiereck, 2017 describes the absorbed wave energy as follows:

$$absorption = \frac{1}{8}\rho g H_T^2 + \frac{1}{8}\rho g H_R^2 - \frac{1}{8}\rho g H_I^2 \tag{2.25}$$

2.2. Bed and bank erosion

2.2.1. Natural banks

Bed, banks and shores are the border between water and soil. As indicated in Figure 2.21, river, channel or lake banks form a rich system with large flora and fauna diversity. A bank facilitates the possibility for species to migrate between land and water and contributes to a healthy and clear water system.

Figure 2.21: Flora and fauna at banks (Waterbeheer, 2009)

Two main types of natural banks are distinguished:

- Dynamic banks, which are found along streams, creeks and rivers. The shape of the banks is determined by discharges, flow velocities and fluctuating water levels. These banks are dynamic and continuously experience erosion and sedimentation. In a highly dynamic only few species can live, but the number of organisms per species will be high (Schiereck, 2017).
- Mildly sloping banks, which are found at lakes, channels and ditches. Because of the mild slope there is abundant space for species. Therefore, these banks are characterized by a great diversity of flora and fauna (Waterbeheer, 2009). Many species can live in a moderately dynamic area such as a mildly sloping bank, but the number of organisms per species will be small (Schiereck, 2017).

If an area is too dynamic, nothing can live. An example of the latter is a beach, where waves break and the environment demands so much of organisms that it is not suitable for plants or animals as a habitat (Schiereck, 2017).

2.2.2. Erosion of natural banks

Under hydraulic loads natural banks can suffer severe erosion. An example is shown in Figure 2.11. Duró et al., 2020 describes the process of erosion of natural banks at navigational channels as a cycle. Currents and wave impact cause soil entrainment at the lower bank. This steepens the bank. At some point the bank becomes unstable and mass failure occurs. A ground wedge or a slump-block is then deposited at the lower bank. The slump-block is partly entrained in the lower bank. This will form a terrace. The rest of the slump-block is removed by the current if the sediment carrying capacity of the channel is large enough. The bank erosion cylce is shown in Figure 2.22.

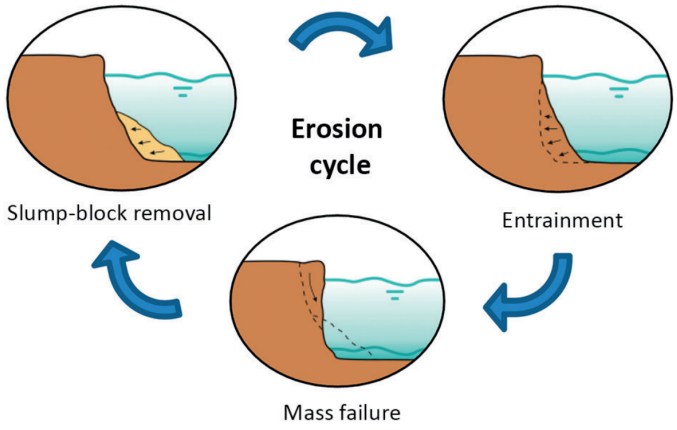

Figure 2.22: The cycle of bank erosion (Duró et al., 2020).

Verheij, 2000 describes the development of a cross-section of natural banks along navigation channels after removing the hard bank protection. The different phases are shown in Figure 2.23. At t_0 the hard bank protections are removed until a depth of h_0. After this, the erosion starts as the natural banks are directly subject to (ship) waves and flow velocities. At t_1 the upper bank has retreated and a terrace has developed due to the process described above. The terrace changes the hydraulic loads on the banks. Waves are attenuated and the flow that reaches the bank is decelerated. Therefore, the retreat of the upper bank slows down. At t_2 a slumb-block has been deposited at the lower bank. The slumb-block protects the upper banks, making it less exposed to hydraulic loads. At t_3 the slump-block has been eroded by the flow and the upper banks are exposed again. Eventually an equilibrium is reached that ensures a more or less stable bank situation.

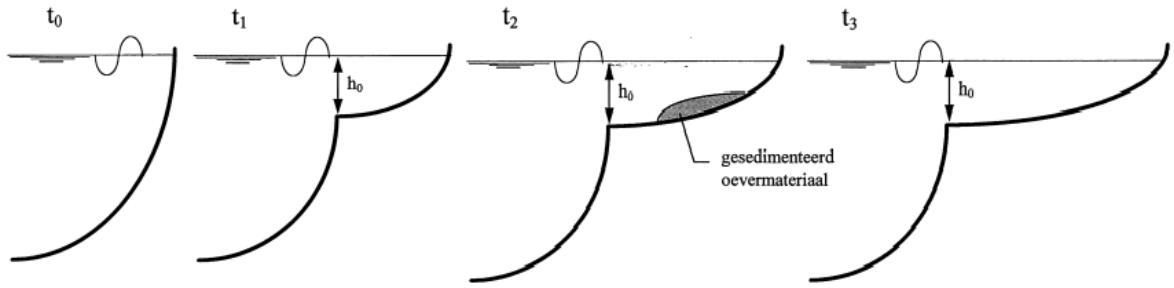

Figure 2.23: Development of a cross-section of a natural bank at a navigation channel (Verheij, 2000).

Verheij, 2000 developed a model called BEM, to model bank erosion of unprotected banks due to secondary ship waves. The cross-section of an arbitrary eroding bank is schematized as in Figure 2.24.

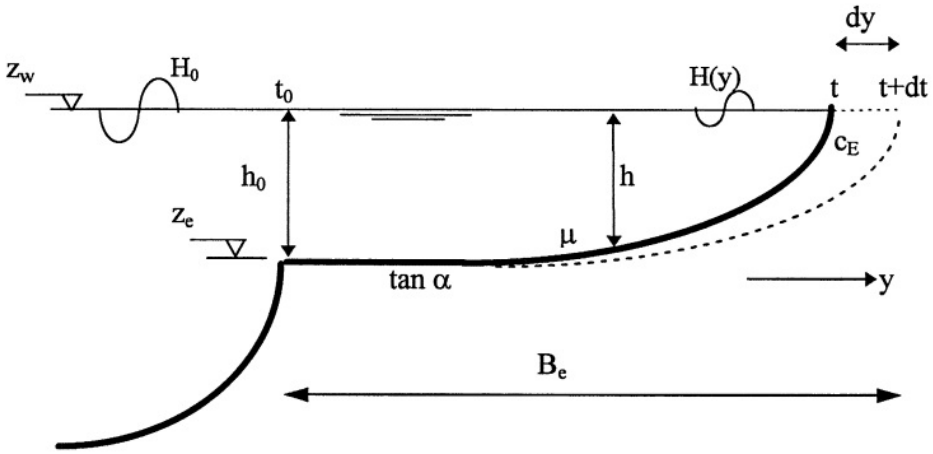

Figure 2.24: Bank erosion schematized by Verheij, 2000.

In this schematization the following parameters were defined:

- Be: the width of the eroded bank in m.
- $tan\alpha$: the slope of the terrace.
- H_0: the incoming wave height at y_0 in m.
- μ: the parameter for wave attenuation of the incoming wave at the foreshore in 1/m. Additional wave attenuation by for example a detached breakwater or a strip of vegetation can be incorporated in the parameter.
- c_e: is a coefficient for the erodibility of banks in 1/ms. For heavy non-erodible bank protections c_e typically has a value of 0. For non-cohesive banks such as sand banks the order of magnitude of c_e is 10^{-3}.

The BEM model estimates the width of the eroded bank Be with Equation 2.26.

$$Be = \frac{1}{2\mu} ln(2\mu \cdot c_e \cdot H_i^2 \cdot t + 1) \tag{2.26}$$

- t: the wave exposure time of the bank for a certain period in s given by $T \cdot N \cdot n$.
- T: the period of secondary ship waves in s.
- N: the frequency of ship passing.
- n: the number of significant secondary waves per ship passing.

Duró et al., 2020 elaborates extensively on the limitations of the BEM model. First of all, it should be noted that the BEM model neglects primary ship waves. Primary ship waves can also have a significant contribution to bank erosion (Schiereck, 2017). Next to that, users of the BEM model have a high uncertainty when choosing input parameters. For example: it is uncertain which value for c_e applies to the bank that is analysed. Also, the slope of the terrace that is formed during the erosion process should be chosen deterministically. The choice for the slope of the terrace influences the wave dampings parameter μ. The models output is highly sensitive for the value of μ. This is illustrated by the plot in Figure 2.25 that shows the upper bank retreat is modelled for 10 years for different values of μ. A large difference in the retreated distance of the upper bank can be observed for the different values of μ. Lastly, the phenomena of bank erosion is highly schematized because of the following assumptions: a fixed lower bank and water level, the bank consists of homogeneous soil, a longshore uniform bank profile.

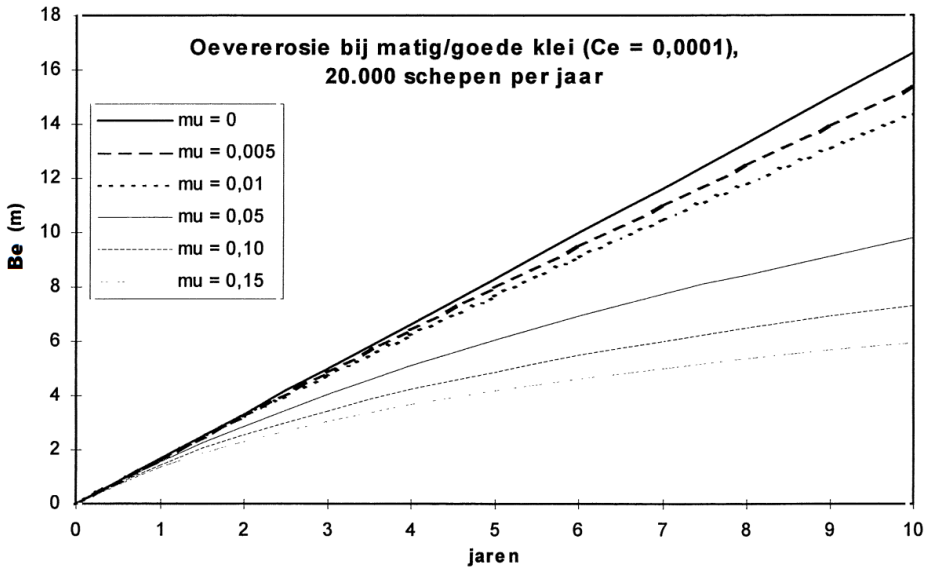

Figure 2.25: Example of BEM: Upper bank retreat in 10 years with $N = 20000$ per year, $Ce = 0.0001$ and various values for mu. Verheij, 2000.

Duró et al., 2020 observed the growth of embayments at navigational channels due to ship wave induced bank erosion. Four types of embayment growth are distinguished. Type a: uniform retreat besides initial perturbation. Type b: symmetric embayment growth. This was mainly observed between trees. Type c: asymmetric embayment growth. Type d: asymmetric embayment growth with a certain irregularity. The types of embayment growth are illustrated in Figure 2.26. In the most erodible stretches that Duró et al., 2020 encountered with his field measurements, the terrace presents mild slopes of 1:25.

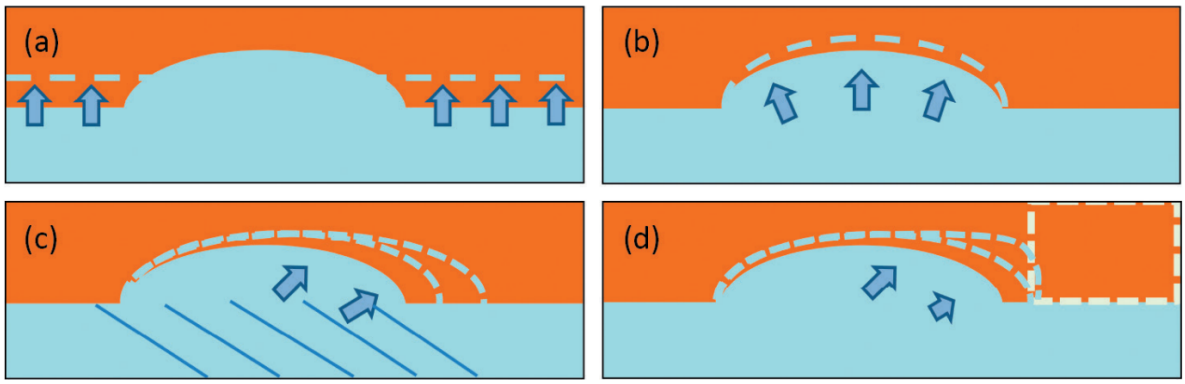

Figure 2.26: "Types of bank retreat observed in the case studies. (a) Uniform retreat besides initial perturbation. (b) Symmetric embayment growth. (c) Asymmetric embayment growth. (d) Irregular asymmetric embayment growth." (Duró et al., 2020).

2.2.3. Bank protections

Schiereck, 2017 gives various hard solutions to increase the strength of banks and to prevent erosion. An elaboration on the types of revetments is given below.

Figure 2.27: Types of hard bank protections. Left to right: Loose rock revetment, placed blocks revetment, vertical sheet pile walls, asphalt (Schiereck, 2017).

- Loose rock revetments can be used in almost every case. It however limits the accessibility of the bank. Rock is largely available and it is relatively easy to construct with. It is mostly applied with a geotextile to prevent washout of fine sediment.
- Gabions are loose stones that are packed together into larger elements. Gabions are used when the available stones are not large enough to withstand the hydrodynamic impacts. They are permeable and vegetation can grow through the elements.
- Placed block revetments are stronger and more reliable than loose rock revetments as it is a more coherent structure. However it is relatively difficult to construct.
- Block mats are used when accessibility and aesthetics of the bank play a role. It is a quite costly solution.
- Asphalt is mainly used at shores where wave attack is severe as it is very strong and reliable.The revetment can be executed permeable or impermeable.
- Groynes mainly serve to maintain a certain water depth in a river or to keep high flow velocities away from the banks preventing erosion. Groins can be constructed with various materials.
- Sheet walls are earth retaining structures out of steel or concrete. These type of structures are preferred if space is limited available.

2.2.4. Nature friendly bank protections

When designed properly, hard structures ensure a continuously stable bank. However, as described in Section 2.2.1, banks play an important role in the ecology of the water land system. These hard structures commonly form a hard barrier in which no ecological migration can take place and in which the natural variability of the system is reduced. Therefore, rather than hard, artificial protections such as sheet pile banks or asphalt revetments, gradual, more natural protections are preferred.

In the Meuse River a systematic bank rehabilitation project was initialized, where bank protections were removed along 80 km between 2008 and 2020. Due to limited knowledge the nature friendly bank designs have shown severe erosion under the influence of ship wave attack (Duró et al., 2020), see figure Figure 2.11. The main challenge in the design of stable and erosion resistant banks is to facilitate a natural boundary between land an water for the migration ecololgy. The Civieltechnisch Centrum Uitvoering Research en Regelgeving (CUR) published various types of nature friendly bank protections. A few examples are shown in Figure 2.28 and Figure 2.29.

Vegetation such as reed and other aquatic plants are able to attenuate waves and reduce flow velocities. In particular ridgid vegetation such as reed is effective as a wave load reductor. The effectiveness of reed to attanuate waves depends on multiple variables. For example the number of stalks per m2, the width of the vegetation strip and the angle of incidence of the waves. Next to that reed dies of in the winter and losses 80% of its wave attenuation capacity. Even-though vegetation strengthens the soil, under excessive wave attack vegetation hardly survives and banks are prone to erode (van Batenburg, 2020). Therefore, vegetation can be reinforced. In Figure 2.28 two examples are shown of grow-through construction. Reinforcing the vegetation strengths the roots and ensures a more stable bank. This can be done with several building materials such as loose rock, block mats, gabions or even geotextiles through which the vegetation can grow. CUR, 1999 has determined the viability of reed that grows through various types of textiles. A desired stalk density can be achieved by choosing the right textile. But generally it takes a few year before the desired stalk density has grown (en

Waterbouwkunde, 1993).

Figure 2.28: Grow-through protections or reinforced vegetation (en Waterbouwkunde, 1993).

A load reductor such as a detached breakwater or a fascine fence can reduce the wave energy that reaches natural banks. Between the load reductor and the bank a wet strip prevails. If the wet strip is too wide, wind waves may be induced. With a load reductor banks are less exposed and the ecological migration processes can take place at the transition between water an land.

Figure 2.29: Left: detached breakwater with a wet strip. Right: fascine fences with wet strip (CUR, 1999).

2.3. Wavepool technology

In this section an elaboration is given on the 24/7Waves technology. After that two other wavepools are analysed on their wave generation and wave damping technology.

2.3.1. 24/7Waves technology

The wavepool that is currently in construction in the Brinckhorst is the first full-scale prototype of the 24/7Waves technology. Several physical scale models and numerical models have already been made and evaluated to analyse the performance of the system. But, both the physical scale models and the numerical models have its limitations. Numerical models, for, example experience difficulties simulating the complexity of moving objects, both sub-critical and trans-critical flow, breaking waves and currents (De Schipper, 2007). Next to that, steep waves ship waves are generated with a steepness in the order of H/L = 1/10. The waves propagating over short distance (± 10 meter) over a flat bottom profile. After this they hit a steep instantaneous slope and break. Linear wave theory can not really describe the nearshore development of the wave because of the relatively large wave steepness and the steep instantaneous slope. Even though, extensive studies have been carried out to proof the performance of the technology, testing the prototype with a trial and error strategy will eventually proof its potential.

The 24/7Waves technology consists of a hull that is towed through water in a rectangular closed basin. The hull is towed at a velocity v_s in a linear path in the horizontal plane, creating waves and currents similar like a ship creates. Due to the bathymetry of the basin the wave breaks. Figure 2.30 gives an impression of the top view of the wavepool.

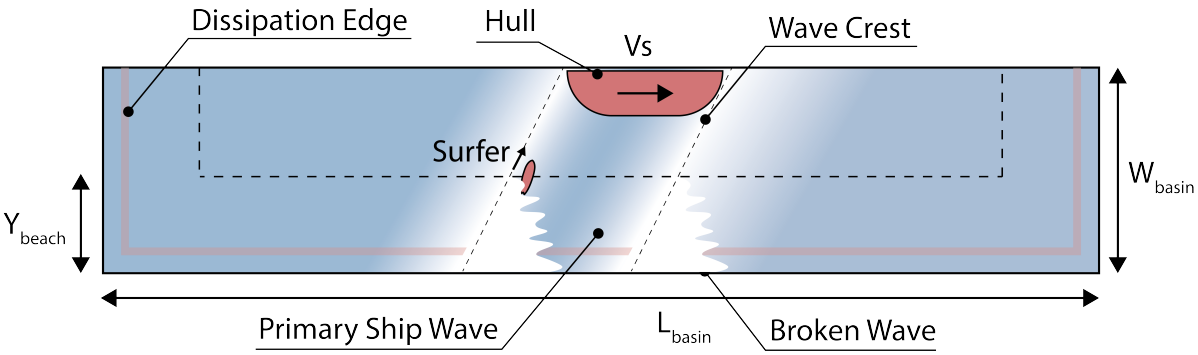

Figure 2.30: Top view wavepool.

Figure 2.31 gives an impression of the dimensions of the cross-section and the different dimensional parameters that are involved. A few important parameters are: the depth at the generation section h_0, distance from the hull to the beach y_{beach}, the width of the beach Y_{beach}, the slopes of the beach a_1 and a_2 and the dimensions and positioning of the edge. The figure also indicates the different sections of the generated wave: the section where the wave is generated, the section where the wave transforms, the section of wave breaking and the section where the wave is dissipated. The broken wave washes over the dissipation edge to eliminate the wave energy from the wavepool. The shape of a generated surfable wave is roughly sketched in the figure. In Appendix C technical drawings are shown of the wavepool that is currently being build in the Binckhorst in The Hague.

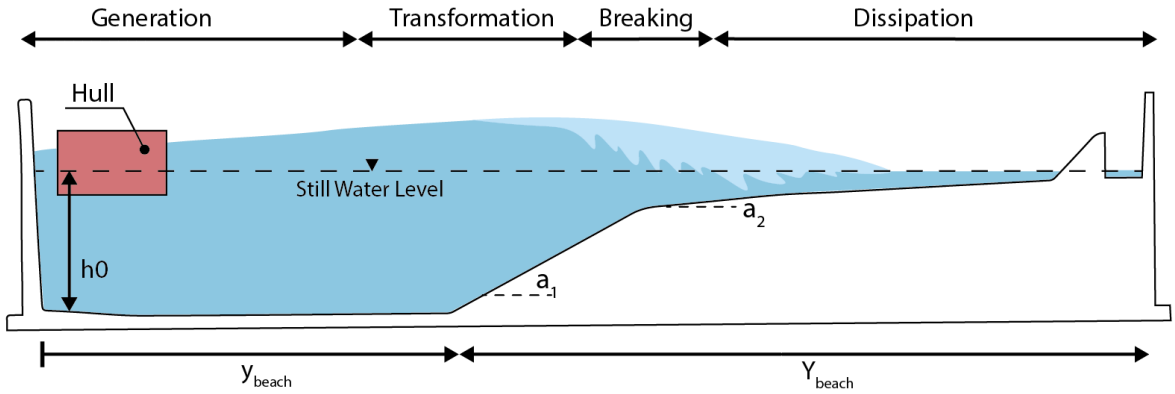

Figure 2.31: Cross-section of the wavepool (Schmied, 2014).

Schmied, 2014 states that the best possible surfable waves are clearly generated if the hull moves in the critical zone. The wave pattern that is identified for a hull moving with critical speed is shown in Figure 2.32. A soliton is formed in front of the pressure source. This is a solitary wave with a crest perpendicular to the pressure source. The soliton travels in the same direction as the hull with a wave speed proportional to both the water depth and wave height (Schmied, 2014). Because the hull moves close to the critical zone the angle of the cusp locus line θ_{cusp} increases. The surfer surfs the unbroken part of the divergent stern wave at the location of the interference cusps. This section of the divergent waves is indicated in blue. Figure 2.33 shows a physical scale model run of a comparable wavepool concept by Schmied, 2014. In this case the hull is towed in a circular path in the critical regime. Schmied, 2014 identifies the generated wave in the model run as a ”smooth high quality” wave.

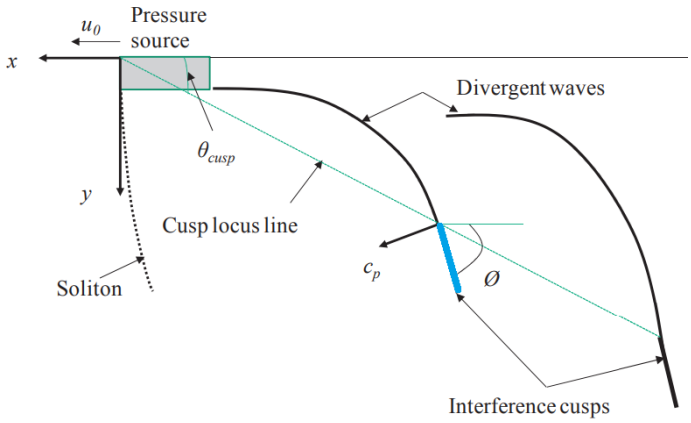

Figure 2.32: Wave pattern behind hull for $Fr_h \rightarrow 1$ (Schmied, 2014) .

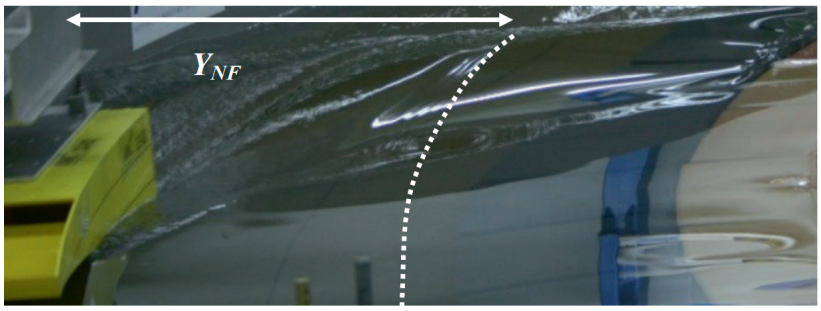

Figure 2.33: Physical model test by Schmied, 2014. Smooth high quality waves are generated at $Fr_h \rightarrow 1$.

2.3.2. Surf Snowdonia wave propagation analysis

Surf snowdonia is a wavepool in Wales. Inspecting Figure 2.34, the wavepool also generates waves along a jetty (1) with a hull. It can be seen that a submerged hull (2) pushes water up while it propagates through the water. A ship wave is formed with a large bow wave, a water level depression and a secondary wave pattern. The bow wave is being surfed breaks (3) and propagates toward the edges. The edge is orientated parallel to the jetty with a distance of 50 m in between the edge and the jetty. At a larger distance from the jetty it can be seen that the wave is unbroken (4) and has a significant smaller wave height than next to the bow. Their technology is considered quite comparable even though, with the 24/7Waves technology the diverging stern wave is surfed.

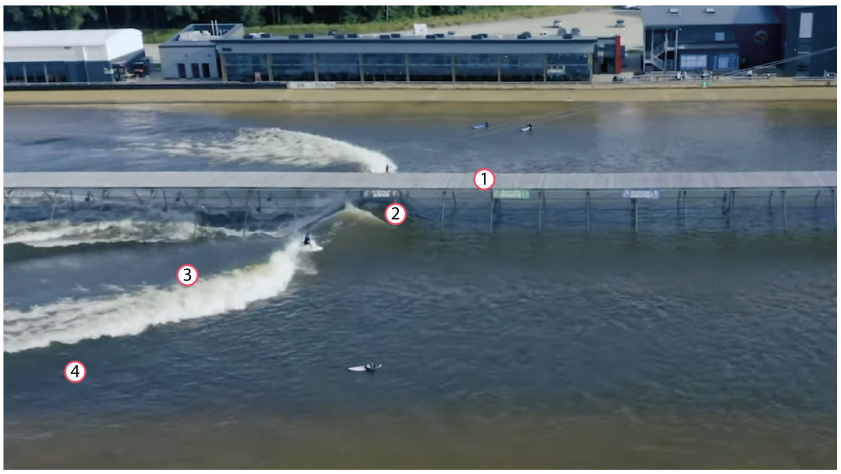

Figure 2.34: Surf Snowdonia wavepool technology and setup.(Maps, n.d.).

A video of the top view of the wavepool allows an analysis of the bow wave propagation. In the upper

panel of Figure 2.35 a top view the surf snowdonia is shown. This gives an impression of the generated bow waves. Screenshots of the video are used to trace along the crests of the bow wave every 3 seconds. In the lower panel of Figure 2.35, the form along the wave crests are shown at eight time instants.

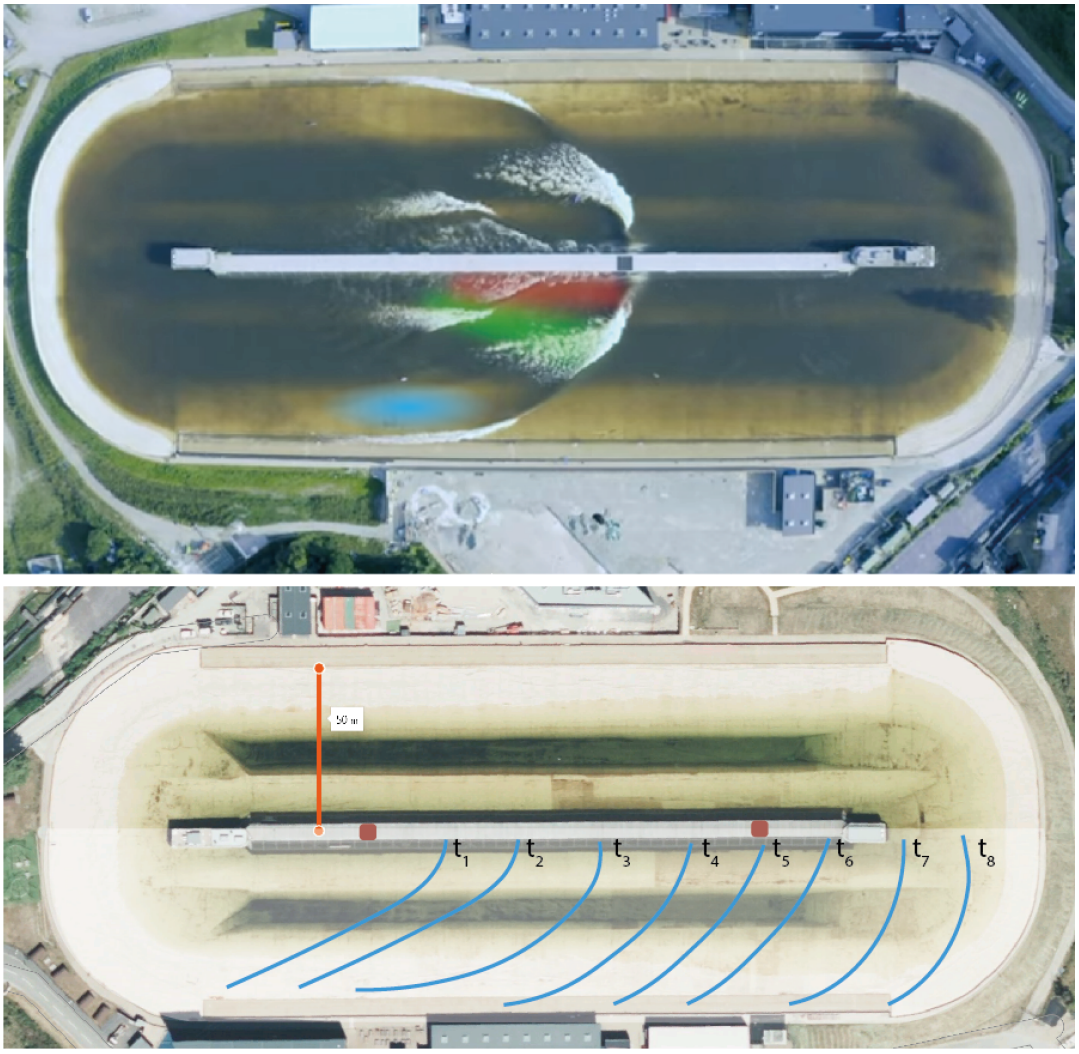

Figure 2.35: Analysis of the wave crests evolution and refraction at the Surf Snowdonia wavepool in Wales (Maps, n.d.).

In the upper panel two different breaker zone can be distinguished. A breaker zone indicated in green and a breaker zone indicated in blue. The green breaker zone the surface roller is bigger and stronger compared to the surface roller at the blue breaker zone. It is reasoned that these breaker zones differ because ship waves diminish with distance from the sailing line (Schiereck, 2017). At a larger distance from the sailing line the wave height diminishes. Waves break in the blue breaker zone with less wave height and thus less energy. Next to that, it is observed that at the blue breaker zone, a line of turbulent water originating from a surface roller has gathered along the edge.

In the lower panel the refraction of the waves can be studied. At the eight time instants the shape along the wave crests barely differ. At time instant t_1 and t_2, the hull starts moving and the wave develops. The shape of the wave crest is quite linear. It is reasoned that the wave height is not large enough that refraction can take place. At time instant t_3 till t_8 refraction can take place which makes the shape of the wave crest more bended. Analysing the angle of the wave crest, it can be seen that, at the location of wave generation (at the jetty), the wave crests are approximately orthogonal with respect to the jetty. At the green breaker the wave has refracted and changed it orientation with ± 45. At the parallel edge the angle of wave incidence is approximately ± 30. It should be noted the shape along the wave crests strongly dependent on the geometry of the bottom profile.

2.3.3. Alaïa Bay wave damping analysis

Alaïa Bay is a Wavegarden wavepool in Switzerland. The wavepool generates waves along a jetty with their pneumatic technology. It is unknown to what extent this technology relates to the 24/7Waves technology. But, because of the fact that their system pumps energy into the waves as they move forward to ensure they maintain a constant height (Wavegarden, n.d.), their technology might be comparable to a wave generated by a hull.

In Figure 2.36 some of the important elements of the wavepool are indicated. The waves are generated at the jetty (1). The wave transforms at the transition from deep to shallow water (2). The waves start to break at the vertical wall (3). The waves propagate radially in the direction of the arrow. When the wave arrives at the edge (4), the complete wave is completely broken along the crest. The wave runs-up and overtops the edge after which the washed over water is collected in the gutter (5). The excess water in the gutter is discharged into the basin via one single opening (6).

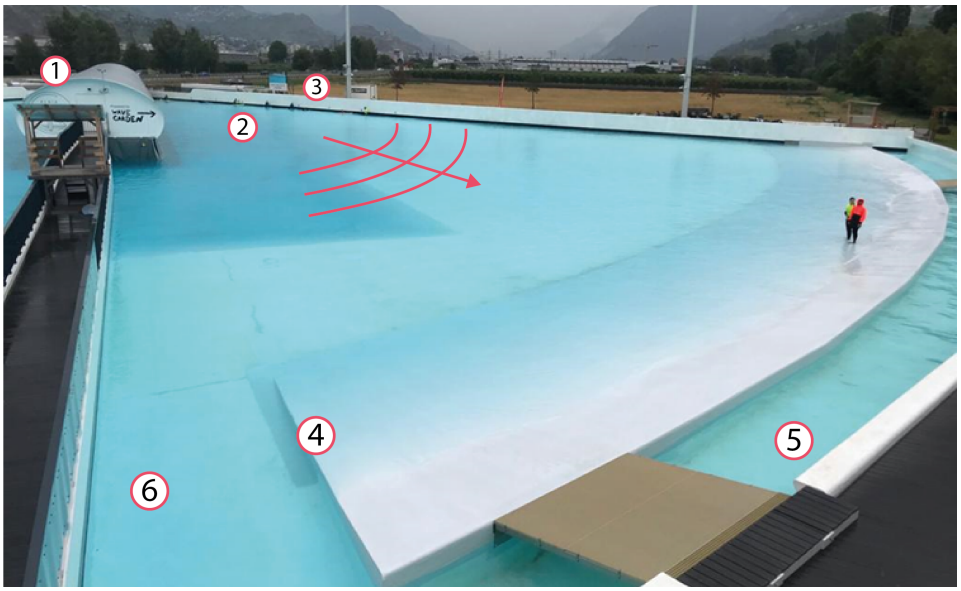

Figure 2.36: Alaïa Bay wavepool setup.

A few other important observations are:

- The still water level is located just below the black line on the wall (2).
- The generated waves propagate over a distance of approximately 100 meters.
- The crest of the edge is located approximately 25 cm above the still water level.
- The slope of the edge is roughly estimated during the site visit to be 1:10.
- The width of the gutter is roughly 3 meters.

Alaïa Bay creates waves for surfers of every level. An expert session offers surfers a steep barrelling wave up to 2 meters. The waves that are generated during 'expert sessions' are the largest waves that the system makes. A single wave motion around the edge at Alaïa Bay during an 'expert session' was filmed and analysed. Several screenshots of the video are shown in Figure 2.37. There is elaborated on the hydrodynamic processes that can be seen in the screenshots.

(a) First time instant: the broken wave propagates towards the edge. A minor wave height decay between the first wave and the second wave (with the surfer). The water level at the slope of the edge and in the gutter can be seen to be located at the still water level. The water in the gutter is relatively calm.

(b) Second time instant: it can be seen that the broken wave runs-up the edge, just before the wave overtops the edge. A certain section of the wave is still unbroken as it runs-up the slope of the edge. The water level in the gutter is not affected yet by the wave run-up.

(c) Third time instant: the broken wave overtops the crest of the edge. Along the edge, water is deposited in the gutter by means of a water jet. The water jet has not reached the vertical wall behind the gutter yet. The water level in the gutter is not affected yet by the wave run-up.

(d) Fourth time instant: the back of the broken wave runs down the slope of the edge back into the wavepool. The water jet is reflected back into the gutter by the vertical wall behind the gutter. This causes the water in the gutter to be very turbulent.

(e) Fifth time instant: the turbulent water in the gutter calmed down. The water level in the gutter is now elevated a little bit above the crest of the edge. The water from the gutter can run down the slope of the edge back into the wavepool.

(f) Sixth time instant: the second wave is running up the slope of the edge. The water level in the gutter is still elevated up to crest level. Because of the elevated water level, less wave energy can be eliminated from the wavepool. It is difficult to see this in the screenshot.

Figure 2.37: Wave damping analysis of a single wave at the Alaïa Bay wavepool in Switzerland.

3

Area study

3.1. Location

The Noorderplas an artificial lake located near Roermond in the North of the Dutch province Limburg. It is part of of the Maasplassen, a network of lakes partly connected to the Meuse river. Originally the Maasplassen are excavation pits for the extraction of gravel. The river Meuse deposited coarse sediment on its floodplains which was mined during low water. Currently the mining of gravel has stopped and the excavation pits have found a new purpose, namely water recreation ("De Maasplassenin Limburg", n.d.). The Noorderplas is located at river km 77 and has an area of 216 ha. The geographical location of the Noorderplas is shown in Figure 3.1. The wavepool will be located on the South shore as indicated by the orange square.

Figure 3.1: The Noordplas at Roermond with the location of the wavepool.

A photograph of the Noorderplas and the location of the wavepool is shown in Figure 3.2.

Figure 3.2: Drone photo of the Noorderplas (van Infrastructuur en Waterstaat, 2020).

3.2. Hydraulic analysis

3.2.1. Water level

Inspecting satellite pictures it can be concluded that the Noorderplas is directly connect to the Meuse river at river km 77. Therefore, water level fluctuations in the Meuse are expected to affect the water level in the Noorderplas directly. Downstream of the Noorderplas, the navigation locks of Roermond and the weir of Roermond regulate the river water levels and guarantee a minimum water level of NAP + 16.70 m. These structures are located approximately at river km 81. This minimum water level is satisfied by Rijkswaterstaat in Figure 3.3. The figure shows the water levels of the Meuse at km 80 for the month April 2022. During this month no extreme events happened. It can be seen that water levels can fluctuate 10 cm within days. Rijkswaterstaat indicates the lightly elevated water level at NAP + 17.00 m. Figure 3.3 also indicates that high water goes up to NAP + 19.00 m and in extreme events even up to NAP + 20.20 m.

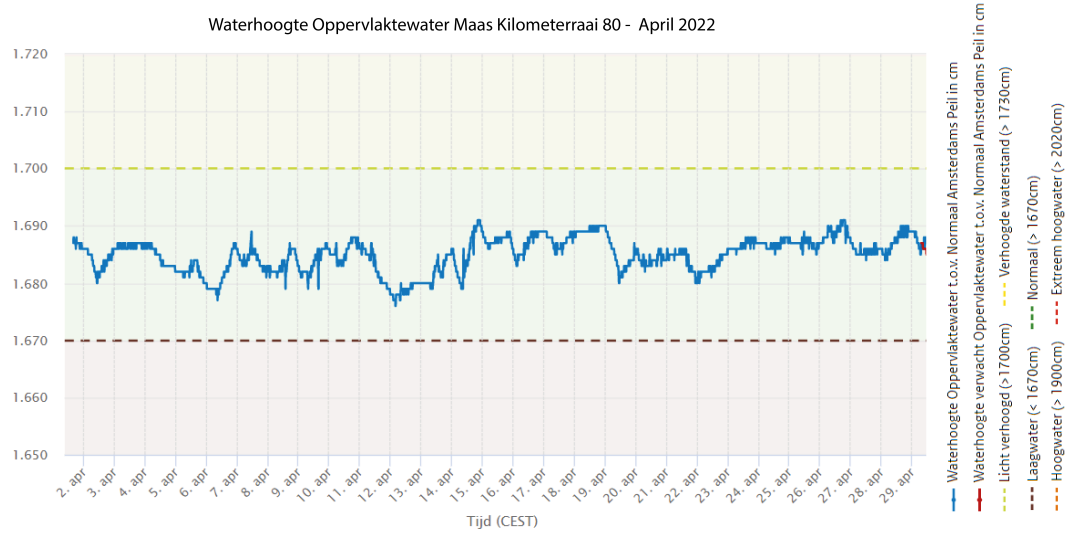

Figure 3.3: Water levels relative to NAP - River Meuse km 80 - April 2022 (Rijkswaterstaat, 2022)

With data from the Rijkswaterstaat an extreme value analysis for the water levels in the Noorderplas is executed. In Figure 3.4 the maximum monthly water levels in the period between 1991 and 2015 are plotted and indicated with the red markers. The average value of the monthly maxima are indicated by the black markers.

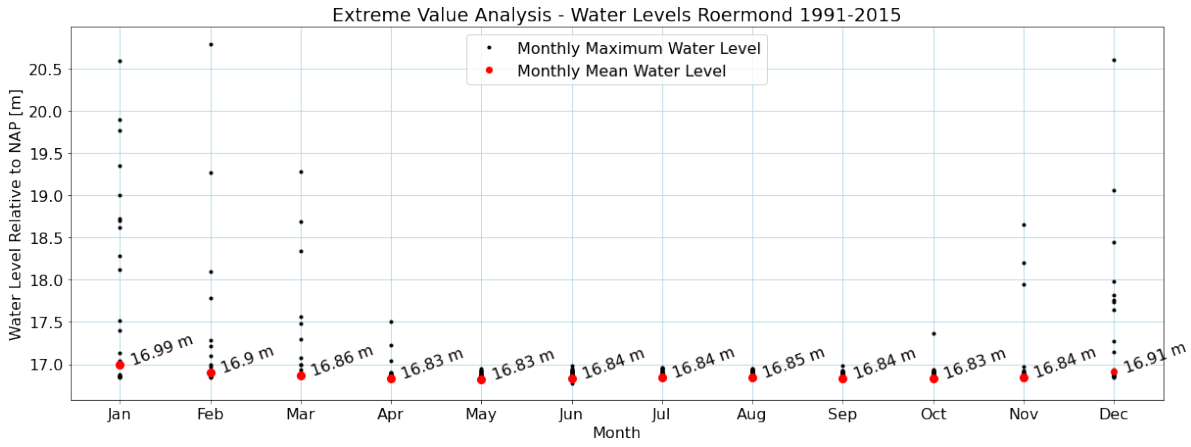

Figure 3.4: Maximum water level (Rijkswaterstaat, 2022)

It can be seen that in the winter months December and January larger water levels are very common. For example in the period between 1991 and 2015 the maximum water level in January has exceeded

more than 15 times the lightly elevated water level of NAP + 1700 cm. In the months April till October this lightly elevated water level is barely exceeded. The past years the Meuse has experienced some extreme river discharges. For example the high water event of July 2021 or March 2019. On aerial footage of the Schepenkring Krekelberg Nautic the Meuse flood of March 2019 was captured. It can be seen that the lake banks of the South shore of the Noorderplas are completely submerged.

Figure 3.5: Flood of the Meuse and high water level in the Noorderplas March 2019 (“Hoogwater Maasplassen Roermond Maart 2019”, 2019)

3.2.2. Waves at the South shore

During a site visit NE wind was of 8 knots was present and no notable wave conditions were observed. Due to the wind no significant wave heights were present. Every once in a while waves of approximately 10 cm were observed generated by navigating ships with moderate speed.

3.3. Lake bed and bank analysis

3.3.1. Soil probes

As mentioned before, the Maasplassen are excavation pits for the mining of gravel. Therefore, it is expected that the soil profile mainly consists of coarse sediment. This is satisfied by various soil probes executed in the lake in 1953 shown in Figure B.2, Figure B.3 and Figure B.4 in Appendix B.

3.3.2. Topography and bathymetry

A field survey has been executed to map the topography and bathymetry of the South shore of the Noorderplas. Appendix A gives a detailed overview of the measurement campaign, the results and the observations. The map of the ground and lake bed level elevations is shown below.

Figure 3.6: Ground and lake bed level elevations South shore Noorderplas

It can be seen in the map that at the nearshore the lake bed profile is relatively longshore uniform. In deeper water more irregularities are present. A pit can be observed in the middle of the map. Three cross-shore profiles are plotted in Figure A.4. At a distance of 20 from the waterline the slopes are almost equal. Between a cross-shore distance of 60 m and 80 m a slope of approximately 1:5 has been determined. As stated before, in deeper water the profiles are more distinct.

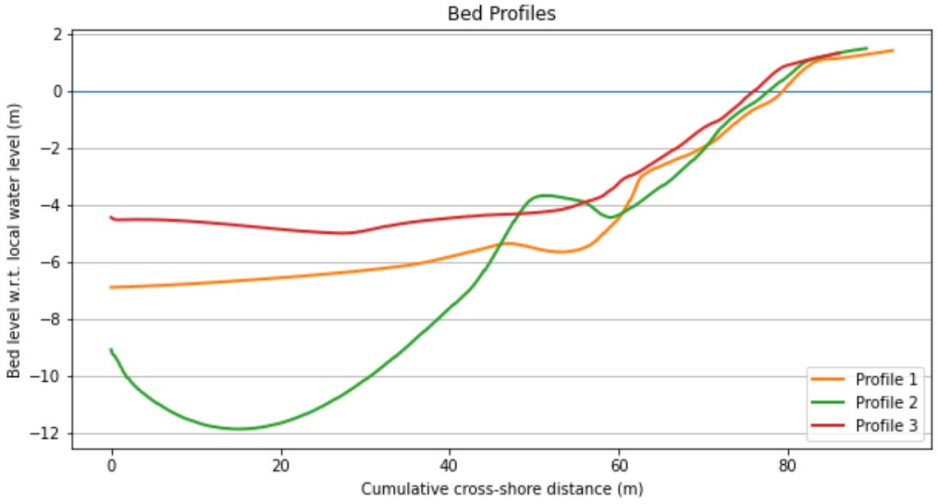

Figure 3.7: Cross-shore profiles South shore Noorderplas.

3.3.3. Morphodynamics

In a conversation with Rogier van Kuijk, the port master of Marina Oolderhuuske, it was mentioned that the excavation marks from the mining machinery are still present in the lake bed even though the mining activities stopped in 1990. These excavation marks form irregularities in the bed profile. From this conversation it is reasoned that barely any transport of coarse sediment takes place. However, it was mentioned by Rogier van Kuijk and observed during the site visits that siltation takes place. Pockets and corners of the lake banks are completely silted up. While mapping the south shore, the foreshore was good accessible, but at the pockets we completely sunk into the mud. It can be seen in Figure A.3 that the pockets and the corners of the lake bed are indeed less deep. The material encountered at these locations was muddy and silty.

3.3.4. Lake bed sediment samples

To get an understanding on the type of sediment on the lake bed, three sediment samples were taken. During a site visit the lake banks and the shallow water near the banks were visually inspected. The banks mildly sloping and full of vegetation (see Figure 3.8a). It was observed that near the banks the bed consists of rocks or coarse gravel. The layer of rocks is not packed dense. In between the rocks an other sediment type could be observed (see Figure 3.8b).

(a) The lake bank

(b) The nearshore lake bed

Figure 3.8: Visual observation lake bank and bed

In shallow water, the water was clear and the lake bed could be seen until a water depth of approximately 0.5 m. When entering the water at approximately a water depth of 1 m the lake bed became quite soft and muddy. Sediment got suspended in the water column when walking through the water. This indicates an other type of finer sediment.

Sediment sample 1 and 2 were taken in shallow water. At a water depth of approximately 1 meter. As mentioned before, rocks or coarse gravel were found at the top layer near the river banks. This is sample 1 and it is shown in Figure 3.9a. The average grain diameter was visually determined to be approximately 4 cm. At the same location the layer of rocks (approximately 5 cm) was removed and a sample was taken directly under the rock layer. This is sample 2 and it is shown in Figure 3.9b. It consists of a mixture of fine gravel, coarse sand and shells. As shown in the figure the sediment types encountered in sample 2 are separated from the sample to illustrate the diversity of the sediment. It should be noted that when taking the sample the water column got turbid very easily.

(a) Sediment sample 1: Rocks

(b) Sediment sample 2: Mixture of fine gravel, sand and shells

Figure 3.9: Visual observation lake bank and bed

Sample 3 was taken at deeper water. At a water depth of approximately 2 m. It can be seen in Figure 3.10 that the sample is muddy. The sediment is very fine and it is mixed with shells and clams. When taking sediment sample 3 the water got turbid very easily as well.

Figure 3.10: Sediment sample 3: Mud mixed with shells

Analysing these samples and soil probes it is reasoned that the top layer of the lake bed probably is silted up. The top of the lake bed probably consists of a little silt layer with coarse gravel layers underneath.

4

Design study

In this chapter a study is executed for an optimal design of the edge of the reef. The area of interest is the lake bank of the South shore of the Noorderplas. In Figure 4.1 a sketch is made of the conceptual layout of the wavepool. The jetty with the wave maker machinery is located parallel to the lake bank at a distance of approximately 30 meters from the water line. The hull is sketched in the figure with the directions in which it will be moving. The lake bank will be subject to the primary and secondary wave components of surfable ship waves generated by the hull. These waves are obliquely incident from two directions. Figure 2.35 is used to sketch the approximated directions of the wave rays. As indicated in the figure, both rear ends of the wavepool are positioned in the lee of one wave directions. The section of the lake bank directly opposite of the jetty is subject to the largest wave loads from two directions. The focus of this design study will therefore be on this particular section of the lake bank, indicated in red in Figure 4.1.

During operational hours of the wavepool it is desired to generate as much waves as possible during operational hours (Order of magnitude 50-100 waves per hour). This is quite intensive loading of the lake banks comparing it to banks of navigation channels (Verheij, 2000).

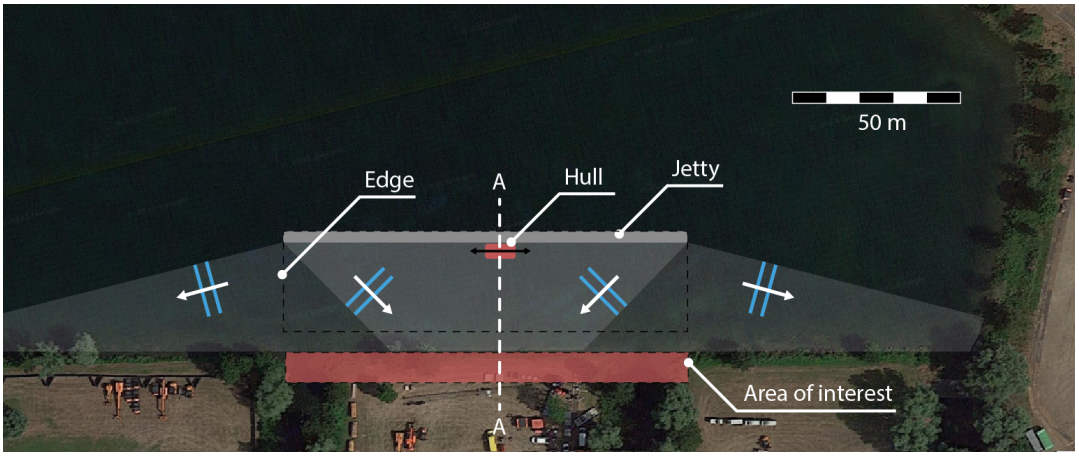

Figure 4.1: Conceptual sketch of the wavepool.

The design of the cross-section in the Brinkhorst is shown in Figure 1.2 and is translated to a lake bank situation shown in Figure 4.2. The reef edge of the wavepool can be seen as a detached breakwater. Normally a detached breakwater is a load reductor that should reflect and absorb wave energy. However, in this case, the detached breakwater should absorb or transmit the wave energy such that it is eliminated from the wavepool. The wet strip corresponds to the gutter system. A wet strip is usually a low energy environment (CUR, 1999). But, in this case it will still be exposed to waves and the lake banks will still have to cope-with significant wave loads. The function of the wet strip will thus be: to damp incoming waves and to discharge the wave over wash to the lake. The lake banks are part of the wet strip. The function of the lake banks is to provide a habitat and migration border for species while it should be able to withstand the remaining wave energy.

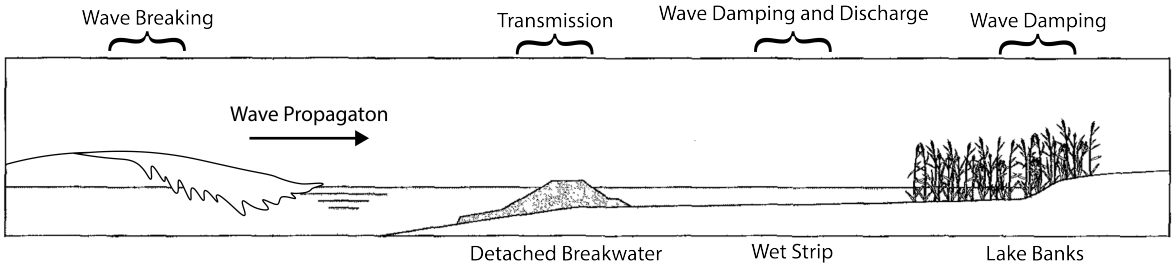

Figure 4.2: Cross-section of the 24/7Waves design translated to a lake bank situation.

In this chapter a design will be made for the dimensions of the detached breakwater, the wet strip. The design study is divided into 4 parts. In part I the boundary conditions for the design are determined. Both the natural boundary conditions of the lake as the generated design wave characteristics are determined. In part II the initial situation is analysed. It is studied what will happen with the lake banks being subject to frequent wave loads. In part III the detached breakwater is designed. A choice will be made for the dimensions and the construction material to maximize wave damping. In part IV the wet strip will be designed. A choice will be made for the dimensions and the construction materials to prevent bank erosion. The strategy of the design study is visualized in Figure 4.3.

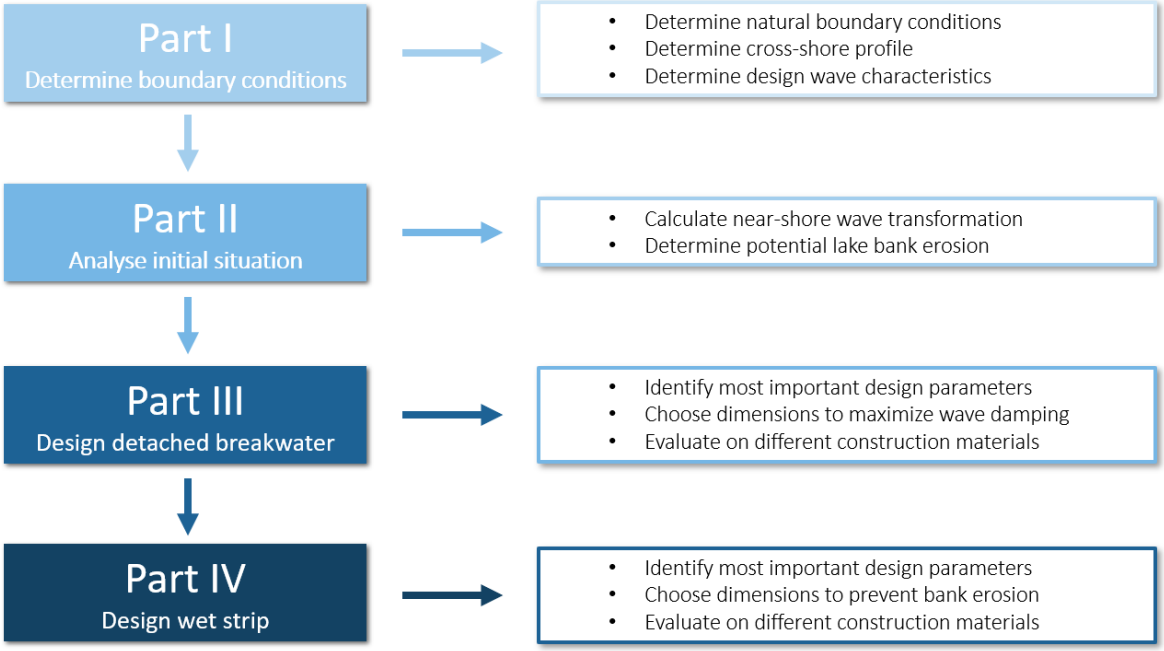

Figure 4.3: Design study strategy.

4.1. Part I: Determine boundary conditions

4.1.1. Determine natural boundary conditions

The most important natural lake conditions to take into account are considered to be the water level variations, the lake bed profile and the lake bed sediment characteristics. An elaboration on the chosen values is given in the table below.

Table 4.1: Assumed lake boundary conditions

Parameter	Value	Reasoning
LWL	NAP + 16.70 m	The lowest water level that is garanteed at the Noorderplas is NAP + 16.70 m (Rijkswaterstaat, 2022).
HWL	NAP + 17.00 m	A boundary condition from 24/7Waves is that the wavepool should be able to preform with water level variations 0.3 m. Thus, the high water level for the design is NAP + 17.00.
DWL	NAP + 17.00 m	The design water level is chosen to be at the HWL. According to the extreme value analysis in Figure 3.4, this seems a reasonable upper boundary for the design and will limit the down time of the wavepool.
Cross-shore profile	Profile 3	As a reference, a cross-shore profile 3 of the Noorderplas is used. Profile 3 slopes gradually with a slope of approximately 1:5 and is considered to be the most cross-shore uniform of all plotted profiles.
Long-shore profile	Uniform	For convenience a long-shore uniform profile is assumed. In reality the long-shore profile is far from uniform
Gravel diameter	$D_{n50} = 50mm$	Rough estimation from sediment sample 1 Figure 3.9
Sand diameter	$D_{n50} = 0.5mm$	Rough estimation from sediment sample 2 Figure 3.9

4.1.2. Determine cross-shore profile

The technical drawings of the cross-section of the wavepool in the Binckhorst, shown in Appendix C, Figure C.1, will guide as a starting point. This reef will be fitted into the natural cross-shore profile of the Noorderplas. An elaboration on the most important dimensions are shown in the table below. The resulting cross-shore profile as indicated as profile A-A in Figure 4.1 is depicted in Figure 4.4. The rectangular edge that is indicated in Figure C.1 is left out of consideration.

Table 4.2: Assumed reef dimensions

Parameter	Value	Reasoning
h_0	2.6 m	In the technical drawings in Figure C.1 the water level is indicated at 2.6 m above the flat beach. In a meeting with Steven Schmied it was mentioned that 2.6 m is the minimum required water depth. Relative to the lowest water level in the Noorderplas, the bottom of the reef will be located at NAP + 14.10 m.
Beach slopes		In the technical drawings in Figure C.1 three different slopes can be distinguished. Each slope runs over a different width. The slopes and widths are derived from Figure C.1 and are shown below.
Slope 1	28°	Derived from Figure C.1
Width 1	3 m	Derived from Figure C.1
Slope 2	5°	Derived from Figure C.1
Width 2	3 m	Derived from Figure C.1
Slope 3	3°	Derived from Figure C.1
Width 3	5 m	Derived from Figure C.1
Horizontal orientation	-	The horizontal orientation of the reef is chosen such that the transition of the reef and the natural profile indicated by the red dot, is in the same water depth as the edge in Figure C.1. Next to that the minimal horizontal width of 17.2 m is met.

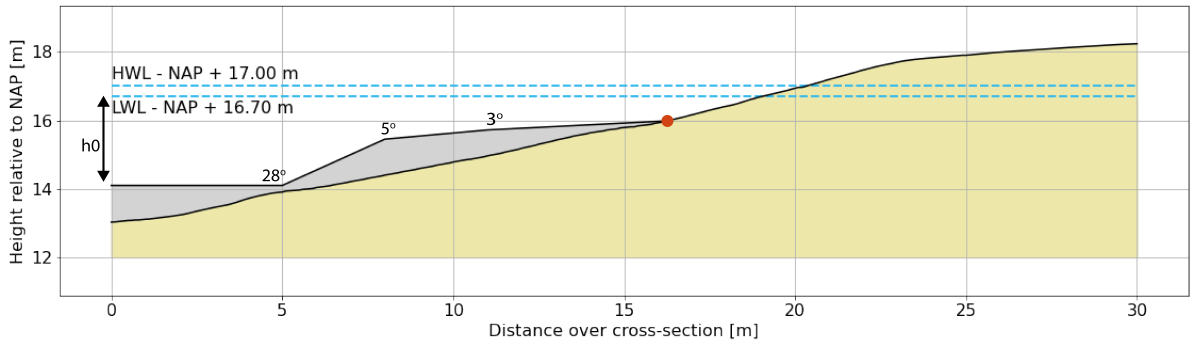

Figure 4.4: Assumed cross-shore profile and reef

4.1.3. Determine design wave characteristics

Often, for the design of hydraulic structures an extreme event is used as starting point of the design. In the case of the wavepool it is difficult to quantify the extreme conditions or design wave conditions. It is namely uncertain what the wave characteristics will be of a wave that is generated by the hull. Next to that, linear wave theory cannot describe the nearshore wave transformation because of the wave steepness and chosen bottom profile (instantaneous transition from intermediate to shallow water).

A certain thing is that the break point of the generated waves is located at some point at the transition from intermediate water to shallow water (between x = 5 m and x = 10 m in Figure 4.4). From this point a broken wave will propagate from the breaker zone towards the edge of the wavepool. Wave height will decay proportionally to the local water depth.

4.2. Part II: Analyse initial situation

4.2.1. Calculate near-shore wave transformation

In Figure 4.5 plot 4 the cross-shore profile A-A is shown. In plot 1 till 3 the near-shore broken wave characteristics are shown. Plot 1 shows the Shields parameter for two different soil types and broken wave conditions. Plot 2 shows the longshore wave induced current. Plot 3 shows the near-shore wave height development.

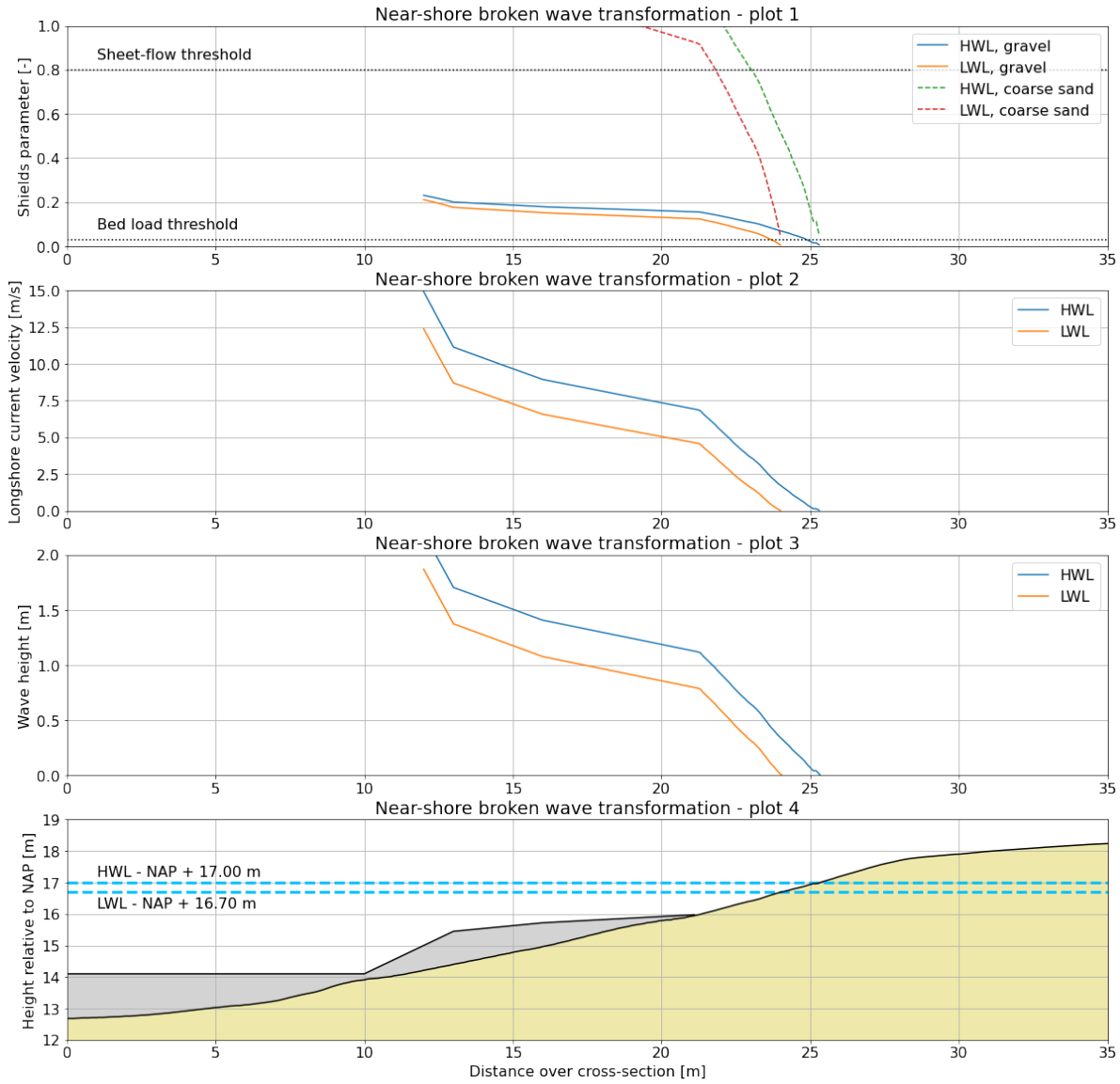

Figure 4.5: Nearshore broken wave development

An elaboration on the approach and the assumptions in making these plots are shown the table below.

Table 4.3: Assumed input variables for the near-shore broken wave transformation.

Wave height - plot 3

Parameter	Value	Reasoning
$H(x)$		Wave height will decay proportionally to the local water depth.
Break point	between x= 5 m and x = 10 m	The break point of the generated waves is located at some point at the transition from intermediate water to shallow water in Figure 4.4).
T	3 sec	It was mentioned by Steven Schmied that the corresponding period for these type of waves is 3 seconds. This is satisfied by the secondary ship wave signals shown in Figure 2.12.
c	$\sqrt{gh}$	A Froude depth close to the critical regime will generate the best possible surfable stern waves (Schmied, 2014). With a Froude depth number close to the critical regime, a upper estimation for the wave celerity is chosen to be equal to the shallow water wave celerity.
L	$c \cdot T$	The relation between wave length, wave celerity and period.
γ	1.1	Analysing the order of magnitude of the Iribarren number ($\zeta = \frac{tan28}{\sqrt{1.5/15}} \approx 2$) the wave design wave will break in a plunging manner. For these type of breakers the range for the breaker parameter is $0.9 < \gamma < 1.2$. A breaker parameter of $\gamma = 1.1$ is deterministically chosen.

Depth-averaged wave induced longshore current - plot 2

Parameter	Value	Reasoning
$V(x)$		Equation 2.12 is used to calculate the depth-averaged longshore wave induced current. Even though the model was calibrated with Figure 2.10, the output seems rather large.
ϕ_0	45°	It is assumed that in a critical regime the stern wave behaves similar as the Featherlet waves. For a Froude depth number close to 1, the incoming wave angle ϕ approaches 90° (De Schipper, 2007). Refraction reduces the incoming wave angle. Using Figure 2.35 a wave angle at the break point of ϕ of 45° is assumed.
c_0	$\frac{gT}{2\pi}$	Deep water wave celerity according to the linear wave theory.
cf	≈ 0.01	Schiereck, 2017 give an empirical relation for the bottom friction factor for turbulent flow over a rough bed dependent, the bottom roughness (r = 2Dn50) and the local wave height.
dh/dx		Plot 4 is used as input for the local bottom gradient.

Shields parameter - plot 1

Parameter	Value	Reasoning
θ		Equation 2.20 and Equation 2.21 is used to calculate the shields parameter for different sediment types.
ρ_{gravel}	$2400kg/m3$	Assumed density of a single grain of gravel
$\rho_{coarsesand}$	$1600kg/m3$	Typical density of coarse sand
D	D_{n50}	See Table 4.1.
ω	$\frac{2\pi}{T}$	The definition of the angular frequency.
k	$\frac{2\pi}{L}$	The definition of the wavenumber. L is calculated with the local shallow water wave celerity and the wave period.

4.2.2. Determine potential lake bank erosion

In plot 1 of Figure 4.5 the Shields parameter is plotted for two sediment types: gravel and coarse sand. The threshold for bed load transport is indicated in the figure. It can be seen that under the generated wave conditions the Shields parameter for both sediment types exceed the bed load threshold. This means that both sediment types are set in motion. For coarse sand the sheet-flow threshold is even exceeded. It is safe to mention that smaller particles might even get suspended in the water column.

With the knowledge that the incoming waves will even set the coarse gravel in motion, it is interesting to analyse the potential bank development. The BEM model is used to get a rough idea of the possible cross-shore profile development of the considered lake bank. The situation in Figure 4.4 is considered without any wave damping measures such as the detached breakwater. Even though the BEM model simplifies the situation strongly it is used to make an estimation of the potential profile development. The inland erosion width Be is calculated with Equation 2.26 and plotted for a period of 5 years in Figure 4.6.

Table 4.4: Assumed input variables for the BEM model.

Parameter	Value	Reasoning
c_e	$0.6 \cdot 10^{-4}$	This value for coefficient for the erodibility of the bank material was validated for the Meuse river banks (Verheij, 2000).
H_i	0.5 m and 1 m	The BEM model estimates the long-term bank profile development. Therefore an average value of the incoming wave height can be chosen. A average incoming wave height is deterministically chosen to be 0.5 meter and 1 meter.
N	200000 per year	The frequency of incoming waves N is chosen to be 200.000 per year. That corresponds to 100 waves per hour, 7 operational hours per day, 300 operational days per year.
n	2	The number of governing waves per ship n is chosen to be 2. This is the same value that the BEM model uses.
μ	0.005 and 0.15	The lowest value for the wave attenuation parameter μ is chosen. This gives an overestimation of the potential bank erosion. It should be noted μ is a time dependent parameter. In the erosion a terrace is formed (Duró et al., 2020) which has a enhanced wave damping effect.

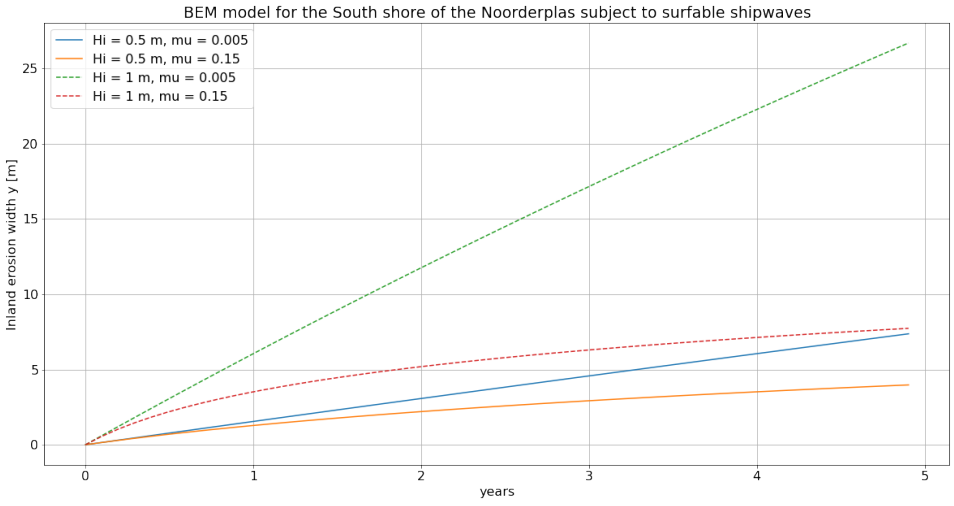

Figure 4.6: Bank Erosion Model for the lake banks subject to surfable ship waves.

Considering the most conservative value for μ and the incoming wave height, with no wave attenuation devices the inland erosion width can be in the order of 20 meters after 5 year. For less conservative

values for μ and the incoming wave height, the inland erosion width can still be in the order of 5 m. It should be noted that these values are a very rough indication of the potential cross-shore profile development. Based on the findings of Duró et al., 2020 and Verheij, 2000, the potential erosion without bank protection and adjusted bank profile is qualitatively sketched in Figure 4.7. The upper bank will retreat land inward and form a steep slope that initiates at the water line. Typically sediment accumulates partly on the lower bank and is partly taken with the current. Also a terrace formed with a slope in the order of 1:25 (Duró et al., 2020). The eroded and accumulated areas are indicated in red. For sediment continuity the eroded area should be equal to the accumulated area.

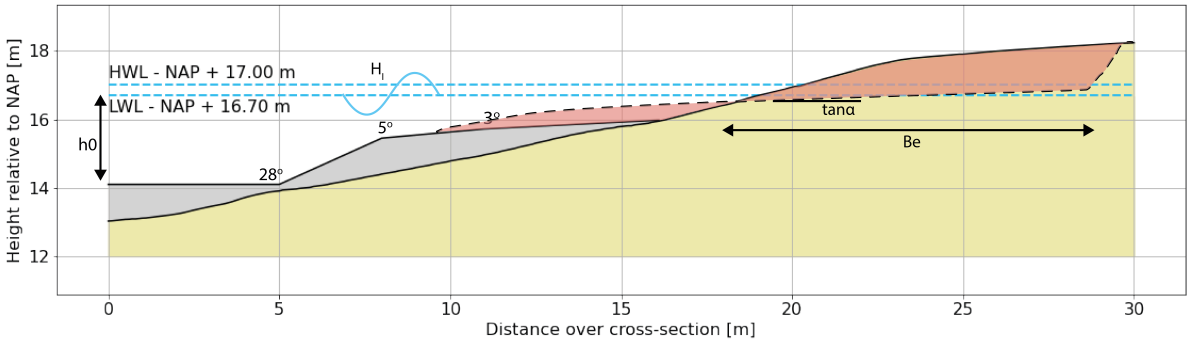

Figure 4.7: Potential cross-shore profile development

It should be noted that the BEM was developed for navigational channels with a current. Sediment that erodes from the upper bank is partly taken by the current. Along the lake bank of consideration there is no current present other than wave induced currents. Sediment can therefore only be transported in longshore direction by longshore wave induced currents. The longshore current calculated in Figure 4.5 seems rather large, but it is undeniable that a significant longshore current will prevail along the lake banks. The CERC method lends itself perfectly to make an estimation of the potential longshore bank development as it only takes into account wave induced longshore currents.

In Figure 4.8 two zones are indicated. Zone 1 is subject to generated waves from two directions. The waves propagate either in eastward or in westward direction. The waves propagate into zone 2. Zone 2 is at both rear ends of the wavepool and is only subject to one wave direction. Zone 1 is thus subject to more frequent wave loads. It is expected that this causes a gradient in sediment transport. Using the CERC method and sediment continuity the long term longshore bank profile is qualitativley sketched in Figure 4.8. It is expected that in the long term an embayment will be formed around zone 1. Sediment is transported by longshore wave induced currents and deposited somewhere in zone 2. This potential longshore lake bank development also corresponds with the fact that generally embayments form along natural navigational channels (Duró et al., 2020).

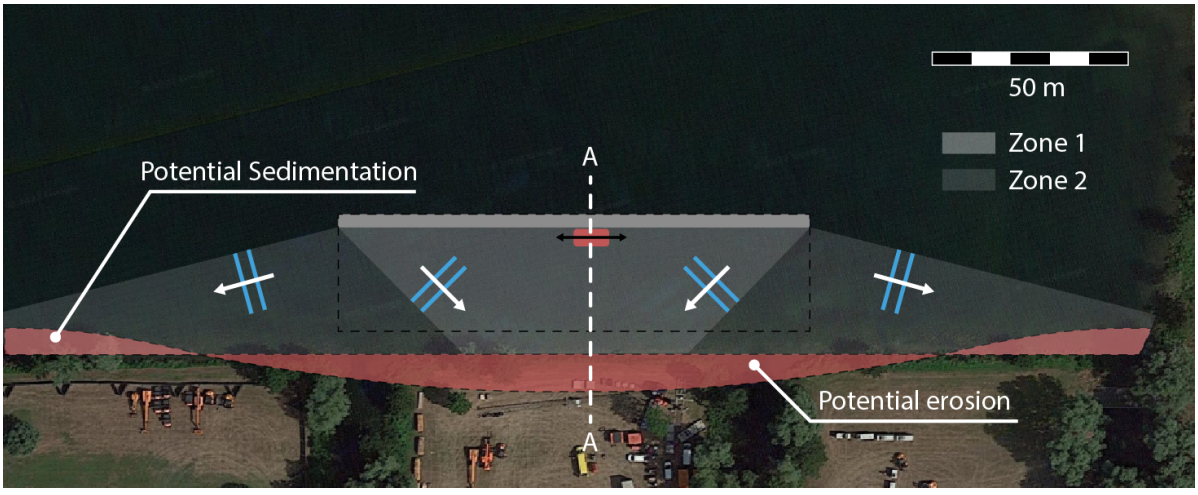

Figure 4.8: Potential longshore bank development

4.3. Part III: Design detached breakwater

First, a decision will be made for the dimensions and the positioning of the detached breakwater. After that loads on the breakwater will be determined. With these loads different building materials will be tested out.

4.3.1. Identify design parameters

The detached breakwater is drawn in the cross-section indicated in Figure 4.9. The most important design parameters are considered the following:

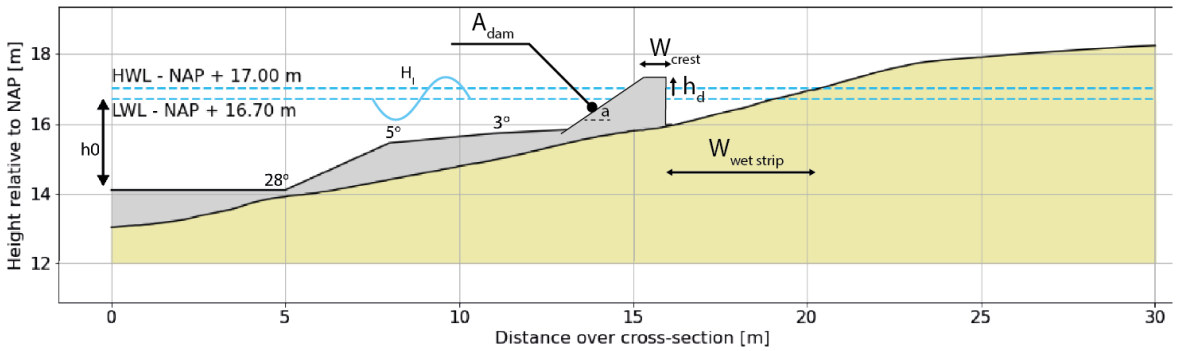

Figure 4.9: Detached breakwater positioned in cross-shore profile A-A corresponding to the technical drawings in Appendix C.

In which:

- h_d: The crest level with respect to the design water level. Positive values indicate emerged breakwaters and negative values indicate submerged breakwaters.
- W_{crest}: The width of the crest.
- $W_{wetstrip}$: The width of the wet strip. Also interpreted as distance between the crest and the design water line.
- α: The slope of the breakwater.
- A_{dam}: The material factor.
- ξ: The breaker parameter defined as $T \cdot \frac{2\pi \cdot H_i}{g}^{-0.5} \cdot tan\alpha$.
- $W_{breakpoint}$: The distance from the crest to the point of wave breaking. This distance is chosen to be 10 m such that it is kept the same as in the technical drawings in Appendix C.

4.3.2. Maximize wave damping

In Section D.1 an elaboration is given on wave transmission of detached breakwaters. Equation D.1 is rewritten such that the crest level with respect to the design water level h_d is a function of the crest width. The incoming wave height H_i is calculated to be a broken wave of 1.2 meter at the location of foot the breakwater ($H_i = \gamma \cdot h = 1.1/cdot1.1$). In this way the transmission coefficient K_t can be kept chosen deterministic. Usually K_t is chosen as low as possible to reduce waves washing over the structure. But for this design study the highest possible value of 0.8 is (d'Angremond et al., 1997) chosen because the wave energy needs to leave the wavepool system.

$$h_d = 2.5H_i \cdot ((\frac{W_{crest}}{H_i}^{-0.31} \cdot (1 - e^{-0.5\xi}) \cdot A_{dam}) - \frac{Kt}{(cos\beta)^{2/3}}) \tag{4.1}$$

With this equation the following possible designs are plotted in a graph. Three other parameters are kept variable: the width of the crest W_{crest}, the angle α and the crest level with respect to the water level h_d. A choice can now be made for the dimensions of the detached breakwater. Schematic examples of the detached breakwater dimensions are depicted in the graph.

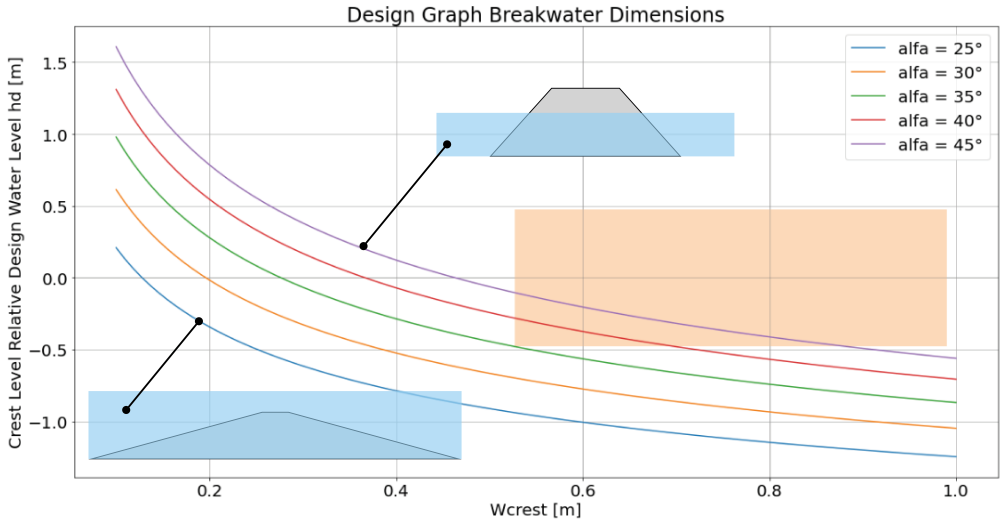

Figure 4.10: Design graph detached breakwater.

Each line represents a possible combination between W_{crest}, α and h_d such that 80% of the height of the design wave is transmitted over the breakwater. To visualize this two breakwaters are sketched in the graph. The orange area indicates the desired range of the the design variables. The width of the crest W_{crest} should be large enough such that people can walk over the detached breakwater. Next to that it is desired that the crest of the breakwater should be located in a range of -0.5 m till 0.5 m with respect to the design water level. Taking this in consideration, a point on one of the lines is chosen within the orange area. The following values are chosen for W_{crest}, α and h_d:

Dimension	Value
α	45°
W_{crest}	0.5 m
h_d*	0 m

*relative to design water level: NAP + 17.00 m

For the chosen dimensions of the detached breakwater shown in the table above, it is analysed to what extend wave energy is transmitted for different water levels and different construction materials. Equation D.1 is plotted in Figure 4.12.

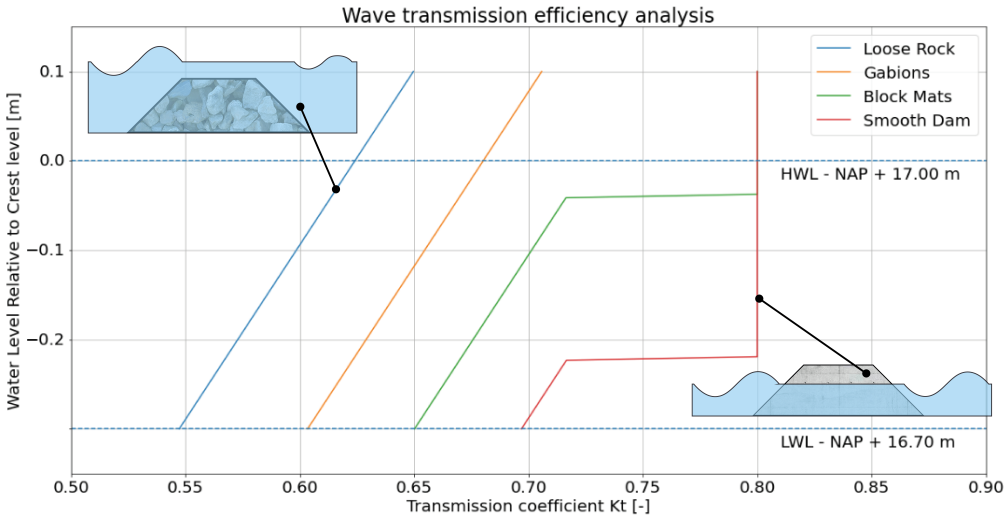

Figure 4.11: Transmission efficiency analysis.

It can be seen that for lower water levels, the wave transmission coefficient K_t decays, independent of the material. This means that for lower water levels less wave energy washes over the structure. This

wave energy is either reflected or absorbed by the structure. It should be noted that for the performance of the wavepool it is quite important to quantify the wave energy that is reflected and the wave energy that is absorbed by the structure. The transmission coefficient does not say something about this.

The different situations regarding the construction material, water level and wave transmission is visualized by sketches in the graph. A breakwater with loose rock is less efficient in transmitting wave energy than a smooth dam.

4.3.3. Evaluation on different construction materials

In this section the possibilities for the use of different construction materials will be explored. A first order estimation will be made for the required dimensions of different construction materials.

Smooth dam - Prefab element

A prefab element can be used for the construction of the detached breakwater. For example a prefabricated concrete element or a gabion is brougth to position and is sunk off to the lake bed. Under wave induced fluctuating water levels a prefab element should be stable against rotation. The resisting moment should be larger than the driving moment as shown in the equation below. The factor γ indicates the safety margin.

$$M_{driving} \cdot \gamma < M_{resisting} \tag{4.2}$$

The following situation is assumed:

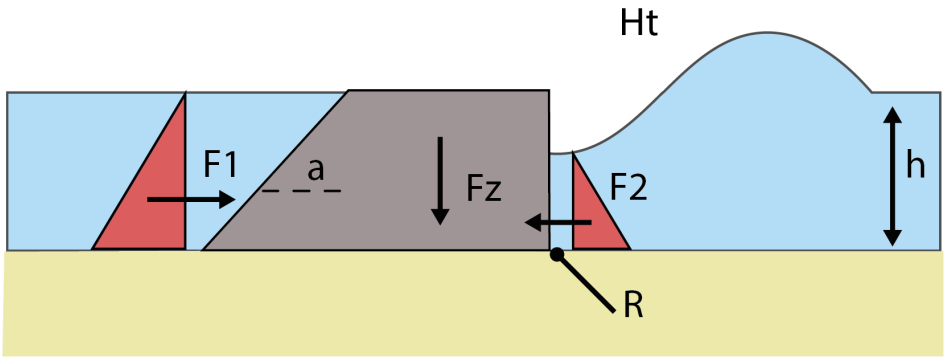

Figure 4.12: Assumed situation: Detached breakwater as a prefab element.

With the following assumed values:

Table 4.5: Assumed values to determine the thickness of the impervious layer

Parameter	Value	Reasoning
ρ_w	1000 kg/m3	-
$\rho_{concrete}$	2400 kg/m3	-
ρ_{gabion}	1440 kg/m3	The density of solid rock with a porosity of 0.4 (CUR, 1999).
h_1	0.9 m	This is the water depth at the detached breakwater derived from Figure 4.4.
H_t	0.9 m	Assuming a transmission coefficient K_t of 0.8
h_2	0.45 m	h_1 minus the amplitude of the transmitted wave.

,

Applying the assumed situation to Equation 4.2 the following relation is retrieved:

$$\frac{1}{3}\rho_w g h_1 \cdot \gamma < \frac{1}{3}\rho_w g h_2 + g(\rho_{material} - \rho_w)(0.18h_1 + 0.45h_1^2) \tag{4.3}$$

A safety factor of γ = 2.9 is found for concrete and γ = 1.1 for gabions. Taking in consideration additional wave impacts at the front of the detached breakwater a gabion structure might be instable against rotation. The margin for the safety factor for concrete is considered sufficient if wave impacts at the front of the breakwater are included.

Smooth dam - Concrete canvas

Concrete canvas is an impervious, soil retaining cementitious composite mat (“Erosion control”, 2022). The main loads that an impervious layer on the detached breakwater would experience under wave loads are: uplift due to fluctuating wave pressure and wave impact induced stresses that exceed the strength of the material (Schiereck, 2017). The layer can withstands these loads by sufficient layer thickness and stiff subsoil. A required thickness will be determined for the concrete canvas to withstand these loads. The following situation of the detached breakwater is assumed:

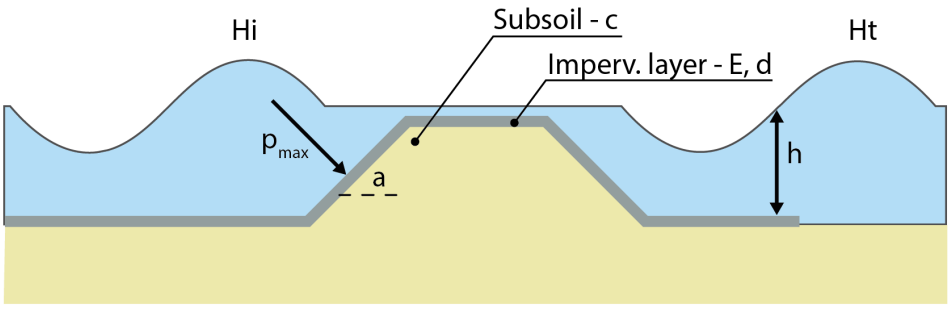

Figure 4.13: Assumed situation: Detached breakwater with concrete canvas

The following values are assumed:

Table 4.6: Assumed values to determine the thickness of the impervious layer

Parameter	Value	Reasoning
H_i	1.2 m	as calculated in Section 4.2.1
H_t	0.9 m	Assuming a transmission coefficient K_t of 0.8
p_{max}	0.2 MPa	The wave impact p_max is given by $8\rho_w gH \cdot tan\alpha$
h	1 m	Assumed minimal required water depth of the wet strip
E	1.6 GPa	Determined by Jun et al., 2020
c	100 MPa	A stiff layer on a soft soil gives large stresses, therefore it is recommended to apply concrete in combination with a stiff soil (Schiereck, 2017). 100 MPa is a typical value for well compacted sand.
a	45°	As determined in the section above.

An elaboration on the theory for assessing the minimal required layer thickness is shown in Appendix D. Rewriting Equation D.6 towards the layer thickness, a minimum required layer thickness of 0.25 m is found to prevent uplift. Water depth and wave length largely influences the required layer thickness. For a wavelength of 8 m for example, the required layer thickness reduces to 0.15 m. After wave transmission the wave length might reduce. It should therefore be noted that the determined minimal required layer thickness of 0.25 m is therefore a very conservative value. .

Determining a failure stress with Figure D.2 a value of 0.2 MPa for the assumed values for the elasticity modulus E and the subsoil stiffness c. Now a comparison can be made with the wave impact induced stresses. The failure stress is a factor 10 larger than the wave impact induced stresses independent of the layer thickness. Therefore, it is unlikely that the concrete canvas will fail due to wave impact. Failure against uplift is considered governing.

Loose Rock

An elaboration on the theory for assessing the minimal rock size is shown in Appendix D. According to Schiereck, 2017 the stern wave is governing for the stability of loose rock on a slope. For the

determination of the minimal required rock size, the following values are assumed:

Table 4.7: Assumed values to determine minimal required rock size

Parameter	Value	Reasoning
z_{max}	1.2 m	The stern wave is the wave that is being surfed. At the detached breakwater a height of 1.2 m is determined in Section 4.2.1
Δ	1.8	With ρ_w = 1000 kg/m3 and ρ_{rock} = 2800 kg/m3 the relative density becomes 1.4
α	45°	As determined in the section above.
R_c	0.1	The crest is located 10 cm below the design water level
$s0_p$	0.1	With the assumed values for the design wave in Section 4.2.1 the offshore wave steepness becomes 0.1

With the assumed values above and the Hudson approach shown in Equation D.2 the minimum required stone diameter is calculated to be 0.37 m. Correcting this for low crested structures that transmit wave energy with the van der Meer approach shown in Equation D.4, the minimum required stone diameter becomes 0.3 m.

4.4. Part IV: Design the wet strip

4.4.1. Identify design parameters

The function of the wet strip is to discharge the wave over wash to the lake and damp th remaining wave energy. The lake banks of the wet strip should provide a habitat and migration border for species. An elaboration on the most important design parameters for the wetstrip are considered the following:

- $W_{wetstrip}$: the width of the wet strip.
- $d_{wetstrip}$: The depth of the wet strip.
- The type of protection layer.
- Vegetation stalk density.
- Vegetation width.

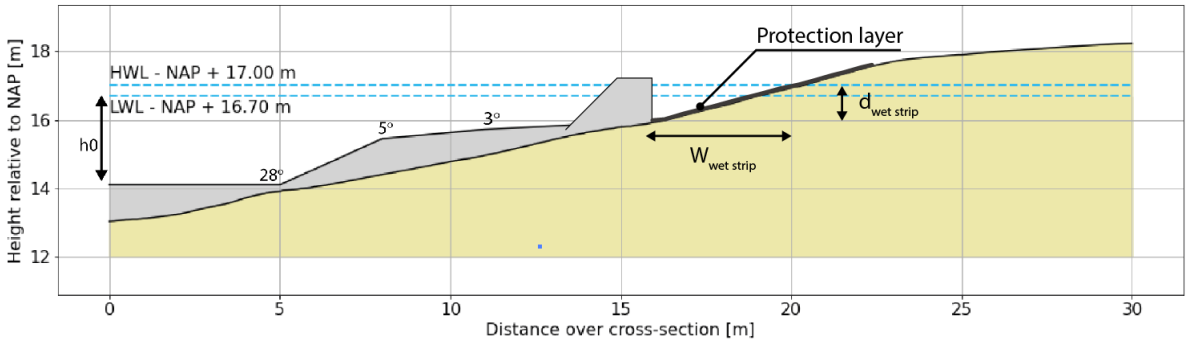

Figure 4.14: Design parameters wet strip.

4.4.2. Prevent bed and bank erosion

A detached breakwater is able to transmit or absorb wave energy to a large extend. It is expected that significant wave energy or turbulent water ends up in the wet strip. With no proper soil retaining bed protection such as a geotextile, fine sediment be suspended in the water column.

The width of the wet strip should be large enough to accommodate the water that is washed after wave transmission. No significant water level elevation may occur after wave transmission because that reduces the wave damping efficiency. Next to that the width of the wet strip should be large enough such that no excessive hydrodynamic conditions prevail at the lake banks.

The depth of the wet strip should be chosen deep enough such that the lake bed is less exposed to wave or turbulent water induced shear stresses which might set the local sediment in motion.

4.4.3. Possible construction materials

Conservative dimensions for the width of the wet strip is chosen to be larger than the wet strip of Alaïa Bay. This is larger than 3 meter. A porous geotextile that can facilitate a grow-through possibility for reed is recommended. Geotextile Secutex171 or Fiber300 are tested by (en Waterbouwkunde, 1993) to have the best penetrability for vegetation. It is recommended that the geotextile should be applied over the whole wet strip at least up to the water line of the design water level. The geotextile can be covered with the local available coarse gravel. It is recommended to use the vegetation as an additional reinforcement of the lake banks. But the stability of the lake banks should not depend on the vegetation due to the capacity loss in the winter. Ridgid vegetation such as reed has a high potential to reduce bank erosion as it has the property to both attenuate waves and strengthen the soil. However, the damping efficiency is reduced up to 80 % in the winter. The larger the stalk density, the larger the wave attenuation efficiency and the more robust the vegetation strip is to die off in the winter. The vegetation provides a natural shelter for lots of species. The larger the vegetation width, the more wave energy will be damped and the less dynamic the hydrodynamic conditions prevail. Calmer hydrodynamic conditions will provide a habitat for more species (Waterbeheer, 2009).

5

Conclusion

The objective of this study is to design the edge and the gutter of the Area X wavepool in the Noorderplas to prevent lake bed and bank erosion. Further design requirements of the edge and the gutter are listed below:

- The edge should be able to dissipate a broken up to 150 mm without reflection.
- Waves originate from both spilling as plunging breakers.
- Varying lake water levels should be taken into account.
- The edge should be aesthetically pleasing.

The final deliverable is a qualitative design for the edge and the gutter of the reef. The most important design parameters to prevent wave reflection and lake bank erosion are listed and a first order estimate for the dimensions and possible construction materials will be given.

5.1. Design approach

The area of interest is the lake bank of the South shore of the Noorderplas indicated as zone 1 in Figure 4.1. The lake bank in zone 1 is subject to the largest expected wave impact that is incident from two directions. The existing design for the reef is taken as boundary condition and is fitted into the cross-shore profile as can be Figure 4.4).

It is difficult to determine the design wave conditions because linear wave theory can not describe the nearshore development of ship waves with a relatively large wave steepness that approach a steep instantaneous slope. Therefore, the design wave is assumed to be a obliquely incident broken wave that is proportional to the water depth with a breaker parameter of $\gamma = 1.1$. This is the starting point for the design of the edge and the gutter of the reef is designed.

With no proper wave damping device it is likely that the lake bank in zone 1 erodes. There is a possibility that in zone 1 an embayment forms with mildly sloping terrace. Due to wave induced shear stresses, sediment up to the local coarse gravel is set in motion. It is expected that sediments accumulates in zone 2 which is identified as a region with milder wave energy.

5.2. Edge of the wavepool

The function of the edge of the wavepool is to eliminate wave energy from the wavepool. Similar to detached breakwaters breakwaters the edge transmits wave energy. Therefore, detached breakwaters are studied for the design of the edge. An elaboration on the most important design parameters for a detached breakwater are considered the following:

- h_d: the crest level with respect to the design water level. To avoid that water flows from the wet strip back into the wavepool, the crest level of the detached breakwater should be positioned above the design water level.
- W_{crest}: the width of the crest. If a value forh_d is chosen, Figure 4.10 can be used to choose a combination for W_{crest} and α that ensures a desired wave transmission efficiency.
- α: the slope of the breakwater.

- A_{dam}: the building material. Wave energy can be eliminated from the wavepool by wave transmission or wave absorption. Whether wave energy is transmitted of absorbed mainly depends on the construction material of the edge. Porous building material will absorb more wave energy than solid structures. Solid structures will transmit more wave energy than porous

Conservative dimensions for concrete canvas or loose rock are determined to be 250 mm and Dn50 = 0.3 m respectively. A prefab concrete dam and a gabion dam appear to be stable against rotation with a safety factor 2.9 and 1.1 respectively.

5.3. Gutter of the wavepool

The function of the wet strip is to discharge the wave over wash to the lake and damp th remaining wave energy. The lake banks of the wet strip should provide a habitat and migration border for species. An elaboration on the most important design parameters for the wetstrip are considered the following:

- $W_{wetstrip}$: the width of the wet strip. The width of the wet strip should be large enough to accommodate the water that is washed after wave transmission. No significant water level elevation may occur after wave transmission because that reduces the wave damping efficiency. Next to that the width of the wet strip should be large enough such that no excessive hydrodynamic conditions prevail at the lake banks.
- $d_{wetstrip}$: The depth of the wet strip. The depth of the wet strip should be chosen deep enough such that the lake bed is less exposed to wave or turbulent water induced shear stresses which might set the local sediment in motion.
- Protection layer: A detached breakwater is able to transmit or absorb wave energy to a large extend. It is expected that significant wave energy or turbulent water ends up in the wet strip. With no proper soil retaining bed protection such as a geotextile, fine sediment be suspended in the water column.
- Vegetation stalk density: Vegetation has a high potential to reduce bank erosion as it has the property to both attenuate waves and strengthen the soil. However, the damping efficiency is reduced up to 80 % in the winter. The larger the stalk density, the larger the wave attenuation efficiency and the more robust the vegetation strip is to die off in the winter.
- Vegetation width: The vegetation provides a natural shelter for lots of species. The larger the vegetation width, the more wave energy will be damped and the less dynamic the hydrodynamic conditions prevail. Calmer hydrodynamic conditions will provide a habitat for more species (Waterbeheer, 2009).

Conservative dimensions for the width of the wet strip is chosen to be larger than the wet strip of Alaïa Bay. This is larger than 3 meter. A porous geotextile that can facilitate a grow-through possibility for reed is recommended. Geotextile Secutex 171 or Fiber300 are tested by (en Waterbouwkunde, 1993) to have the best penetrability for vegetation. It is recommended that the geotextile should be applied over the whole wet strip at least up to the water line of the design water level. It is recommended to use the vegetation as an additional reinforcement of the lake banks. But the stability of the lake banks should not depend on the vegetation due to the capacity loss in the winter.

5.4. Recommendations

Analysing the dissipation of the normally incident waves at Alaïa Bay, it can be seen that very turbulent water is deposited in the gutter as the wave overtops the edge. At the Noorderplas, lake banks are very likely to erode being subject to similar wave loads. Intuitively it is expected that a short instantaneous edge is not able to reduce these wave loads sufficiently. Analysing the dissipation of the obliquely incident waves at Surf Snowdonia, it can be seen that they approach the edges quite calmly because of refraction and a large dissipation distance (order 50 m). Therefore it is recommended to explore the possibilities for a more mildly sloping dissipation edge (order 1:10 - 1:25) as shown in Figure 5.1. It is recommended to determine the wave run up, wave over-topping and determine the discharge that ends up in the wet strip. The width and depth of the wet strip should be chosen such that turbulent water does not reach the lake banks.

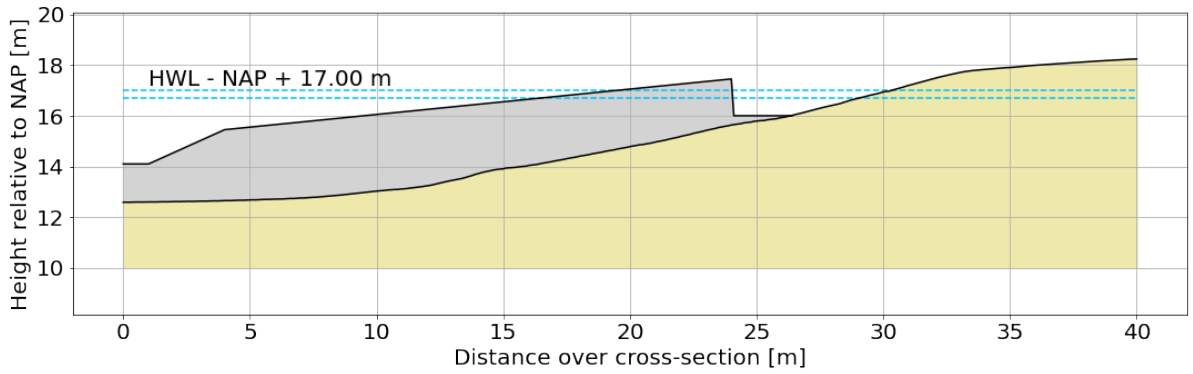

Figure 5.1: Mildly sloping reef for follow up research

The Maasplassen are excavation pits of former gravel mining activities. This means that locally, abundant of coarse sediment is available that can be used as construction material. Continuous dredging works are executed in the Meuse river and surrounding waterways that collect gravel (“Baggerwerkzaamheden Maas”, 2021). It is recommended to explore the possibilities to construct the detached breakwater (maybe even the complete reef) by means of a ’sustainable’ cut and fill strategy with the local available gravel. In the first place because rough and porous surfaces are able to absorb wave energy effectively. It is likely that the gravel won’t be stable under the prevailing wave conditions. But in the form of a gabion, the gravel is packed as a coherent element. Next to that, gabions provide space for vegetation to grow through.

Lastly, it is recommended to explore the possibilities for an adaptive design. Several physical scale models and numerical models have already been made and evaluated to analyse the performance of the wavepool and the wave damping system. But, both the physical scale models and the numerical models have its limitations when describing the reality. Testing the full scale prototype with a trial and error strategy will eventually proof its potential. A safe way of exploring the potential of the full scale prototype is to make the prototype adaptive rather than fixed. For example, choosing adjustable solid elements, different configurations for the wave damping system can be tried out. For varying water levels and different generated waves, different positioning and shapes of the wave damping system can be tried out. In this way, a safe trial and error strategy is realized to explore the potential of the full scale prototype.

References

Baggerwerkzaamheden maas. (2021). https://www.rijkswaterstaat.nl/nieuws/archief/2021/05/boskalis-start-baggerwerkzaamheden-maas-in-gelderland-en-noord-brabant

Battjes, J. A. (1974). Surf similarity. *Coastal engineering proceedings*, (14), 26–26.

Bosboom, J., & Stive, M. (2021). *Coastal dynamics*. https://doi.org/10.5074/T.2021.001

CUR. (1999). *Natuurvriendelijke oevers, belasting en sterkte*. Ministerie van Verkeer en Waterstaat.

d'Angremond, K., Van Der Meer, J. W., & De Jong, R. J. (1997). Wave transmission at low-crested structures. *Coastal engineering 1996* (pp. 2418–2427).

De maasplassenin limburg. (n.d.). https://www.hartvanlimburg.nl/nl/dagje-uit/waterrecreatie-op-de-maasplassen

De Schipper, M. (2007). On the generation of surfable ship waves in a circular pool: Part i: Physical background and wave pool design.

Duró, G., Crosato, A., Kleinhans, M., Roelvink, D., & Uijttewaal, W. (2020). Bank erosion processes in regulated navigable rivers. *Journal of Geophysical Research: Earth Surface*, *125*(7), e2019JF005441.

en Waterbouwkunde, D. W. (1993). *Doorgroeibaarheid van geotextielen*. Ministerie van Verkeer en Waterstaat.

Erosion control. (2022). https://www.concretecanvas.com/

Holthuijsen, L. H. (2010). *Waves in oceanic and coastal waters*. Cambridge university press.

Hoogwater maasplassen roermond maart 2019. (2019). https://www.youtube.com/watch?v=dNTut02UmlQ&ab_channel=SchepenkringKrekelbergNautic

Jun, Z., Wei, X., Xingzhong, W., Peiwei, G., Zhihua, Y., Lihai, S., & Jiang, W. (2020). Application and research status of concrete canvas and its application prospect in emergency engineering. *Journal of Engineered Fibers and Fabrics*, *15*.

Maps, A. (n.d.). Surfing an artificial wave - everything you need to know (surf snowdonia). https://www.youtube.com/watch?v=BCtiJQUqqJo&ab_channel=AwesomeMaps

of Washington, U. (2006). Oceanography - waves.

Pinterest - tamarindo c.r. (2018). https://www.pinterest.at/pin/685743480734689672/

Rijkswaterstaat. (2022). Waterhoogte oppervlaktewater roermond boven. https://waterinfo.rws.nl/#!/details/publiek/waterhoogte/Roermond-boven(ROER)/Waterhoogte___20Oppervlaktewater___20t.o.v.___20Normaal___20Amsterdams___20Peil___20in___20cm

Schiereck, G. J. (2017). *Introduction to bed, bank and shore protection*. CRC Press.

Schmied, S. A. (2014). *Limitations on the creation of continuously surfable waves generated by a pressure source moving in a circular path* (Doctoral dissertation). University of Tasmania and TU Delft.

SurferToday.com, E. a. (n.d.). What is wave diffraction? https://www.surfertoday.com/surfing/what-is-wave-diffraction

van der Meer, J. W., BRIGANTI, R., WANG, B., & ZANUTTIGH, B. (2005). Wave transmission at low-crested structures, including oblique wave attack. *Coastal engineering 2004: (in 4 volumes)* (pp. 4152–4164). World Scientific.

van Batenburg, K. (2020). Modelling of hydrodynamic and erosion processes at vegetated lake shores: Development of a process-based tool for the design of the protection of a lake shore with reed-like vegetation.

van Infrastructuur en Waterstaat, M. (2020). Waterveiligheid vergroten en ontwikkelperspectief creëren. https://magazines.deltaprogramma.nl/deltanieuws/2020/03/waterveiligheid-vergroten-en-ontwikkelperspectief-maasplassengebied-creeren

van Koningsveld, T., Verheij, & de Vriend. (2021). *Ports and waterways, navigating the changing world*.

Verheij, H. (2000). Samenwerkingsproject modellering afslagoevers: Voortgangsrapportage 1999. *Q2529*.

Waterbeheer, S. T. O. (2009). Handreiking natuurvriendelijke oevers.

The wave. (2020). https://www.area-x.nl/the-wave-golfsurfen-roermond/

Wavegarden. (n.d.). Wavegarden technology. https://alaiabay.ch/en/

A

Noorderplas field survey Mapping the topography and bathymetry of the South shore

A.1. Measurement campaign

Parameters of interest

To define the boundary conditions of the lake for the construction of the wavepool and for the future monitoring of the lake banks and bed elevations, a topographic and a bathymetric map of the area is desired. This map must show the ground level and lake bed level elevation with respect to a certain reference level. It is expected that the elevations need to be mapped with at least an order of accuracy of 10 cm. It would be practical if the soil types of the lake bed top layers are measured as well, but this is not considered mandatory.

Measuring & Survey equipment

GPS

The data on the ground level elevation and the water level will be gathered with a GPS. A Leica GS07 GNSS RTK-sensor in combination with a Leica Viva CS15 controller is proposed. These instruments can be moved around to make point measurements of a certain area. The point measurements contain following data: time, GPS coordinates of the point, ground level elevation with respect to a certain reference level and accuracy of the measurement. Usually an accuracy of 1 cm is achieved.

Echo sounder

If available, an echo sounder can be used to measure the distance from the device to the lake bed. Relating this distance to the water level, the water depth can be determined and the lake bed elevation with respect to an desired reference level can be determined.

GPS extension pole

If no echo sounder is available, the measurements will be executed only with a GPS. This will make the mapping of the bathymetry more difficult but not impossible. To reach the lake bed with the GPS rover a extended pole is needed of ± 3 m. From the boat the end of the pole will be placed on the lake bed and the measurement will be collected as normal.

Boat

A small motor boat is sufficient for navigation with the echo sounding equipment.

Mounting system

A system that mounts the echo sounder to the boat is required. The system should keep the echo sounder stationary and in place during navigation. This system is yet to be determined.

Level

A level can be used to determine if the echo sounder is installed correctly.

Clothing

Proper clothing is required for the surveyors. Using a wetsuit the surveyors will be able to execute

their measurements in the water without getting cold. Water shoes will enable the surveyors to walk in shallow water.

Location of interest

The location of interest is the South shore of Noorderplas. At the South shore the wavepool will be constructed covering a area of approximately 1.5 hectares (± 150 m x ± 100 m). The approximate location of the wavepool is indicated in red in Figure A.1. As the exact location of the wavepool is yet to be defined, a margin is chosen around the edges of the approximate location. This will both give slack for the final decision of the exact location of the wavepool and it will make future monitoring of bed and bank erosion possible. The complete area of interest is approximately 8.5 hectares (± 500 m x ± 175 m). Coordinates are indicated in Figure A.1.

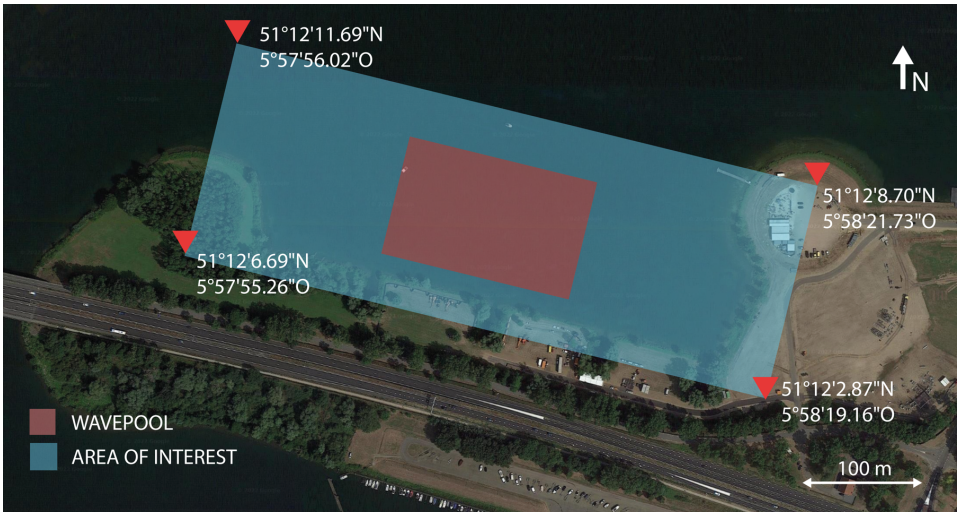

Figure A.1: Area of interest

Measurement strategy

Point measurements from both the GPS and the echo sounder will be done within the area of interest. The area of interest is divided into a grid to gather the point measurements in a systematic way. At each grid point measurements will be taken. Grid cells of 20 m x 20 m are chosen. The locations where the ground level or bed level elevation is expected to vary within short distance,a higher spatial resolution is desired. So around the lake banks a finer grid of 2 m x 2 m is proposed. This has resulted in grid shown in Figure A.2.

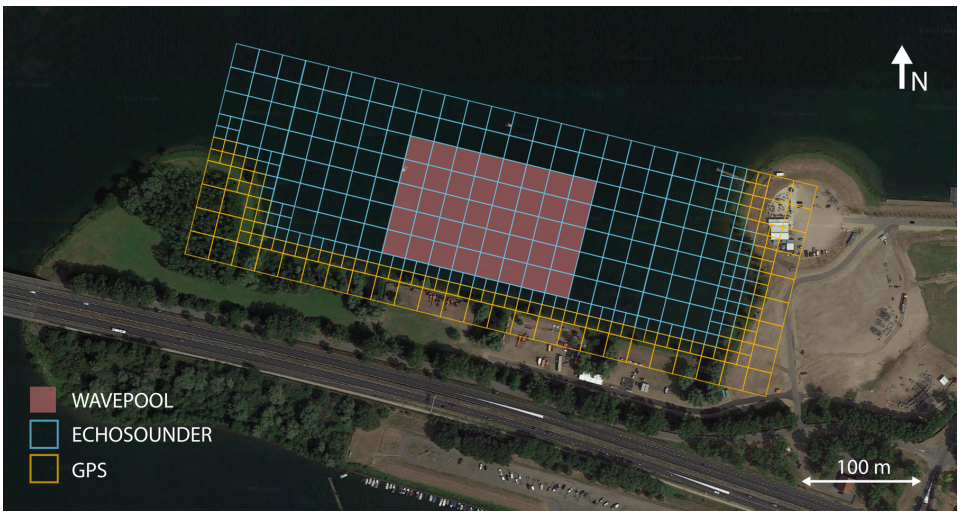

Figure A.2: Proposed grid for the GPS and Echosounder measurements

The yellow grid cells indicate the area that has to be mapped with walking with the GPS. The walking distance to be covered is approximately 4 km. The blue grid cell indicate the area that has to be mapped sailing with the echo sounder. The sailing distance to be covered is approximately 6 km.

Planning & measuring period
Taking into account the approximate sailing and walking distance and a sailing and walking speed of 5 km/h, covering the distance would be possible in 2 hours. Including the time needed for the deployment of the equipment, preparation of the boat and other down time, it is expected that the measurements can be executed in one day. The following days are proposed for the practise session: Monday 23 May, Tuesday 24 May or Wednesday 25 May. The following days are proposed for the field survey: Wednesday 25 May, Thursday 26 May or Friday 27 May. A proposal of the survey planning is shown in Table A.1.

Table A.1: Survey planning

Time	activity
8:00	Arrival at Noorderplas Meet people on site Prepare boat
9:00	Install echo sounder on the boat Startup of the equipment
10:00	Start of bathymetric survey Sail in the pattern of the grid
13:00	End of bathymetric survey Demount the equipment
13:30	Break
14:00	Deploy GPS
14:30	Start of topographic survey Walk in the pattern of the grid
18:00	End of topograpic survey

Weather
It is expected that bad weather such as wind and rain would not decrease the accuracy of the data nor cause trouble while executing the survey.

Practise with equipment
To get acquainted with the equipment it is proposed to a practise survey a few days prior to the survey.

Survey team
For the topographic survey, a team of 2 members is proposed. One member should walk around with the GPS rover and one member keep track of the grid. The same holds for the bathymetric survey. One team member will be in charge of the measuring equipment and the other will be in charge of the sailing.

Data processing
The data points on ground level and bed level elevation is stored in a .txt file. The data is checked for errors and outliers are deleted. The data can be linearly be interpolated and visualized using either Python or in QGIS.

A.2. Evaluation of the field survey

Monday 23 May the measurement instruments and tools were picked up at the TU Delft. With Field Work Coordinator Pieter van der Gaag a practise session was carried out to get acquainted with the GPS device. Thursday 26 May the field survey was executed. At 09:00 the survey team arrived at Marina Oolderhuuske in Roermond where the boat was picked up. The day prior all equipment was

prepared and set apart. Everything went as planned. A little breeze was present but nothing that could really disturb the survey.

From the TU Delft no echo sounder was available. Therefore, the measurements where executed with the GPS device and the extended pole. The plan was to put the pole in the water on the bed level. When the bed level was reached the a point measurement was taken with the GPS. In practise it was not possible to take the point measurements in this way. First of all, it was found that the slope of the foreshore was quite steep. At a distance of approximately 10 meters from the shore the water appeared to be too deep to reach the lake bed with the extended pole. Therefore, a significant percentage of the area of interest could not be mapped. Next to that, it appeared to be very difficult with the wind conditions to keep the boat stationary while taking the point measurements. It takes approximately 2 seconds for the GSP to make a point measurement. While placing the pole on the lake bed the boat drifted away and the pole could not be hold in place.

Luckily, the port master of Marina Oolderhuuske, Rogier van Kuijk provided us an Hawkeye DepthTrax echo sounder. This echo sounder was able to indicate the instantaneous water depth at any place in the lake with a 10 cm accuracy. However, this accuracy was questioned because of a reference measurement. The reference measurement with the echo sounder indicated a water depth of 90 cm while a folding ruler indicated a water depth of 110 cm. The accuracy was a little less than hoped probably because bed vegetation, silt, mud or other soft bed material disturbed the signal. Despite the unknown accuracy of the device, the measurement strategy was changed by making use of the Hawkeye DepthTrax in combination with the GPS. While following the grid shown in Figure A.2, GPS point measurements where taken and simultaneously the depth was measured with the Hawkeye DepthTrax. The point measurements where numbered and the corresponding water depth was noted down in an excel file. With the reference measurement of the water level at NAP + 16.93 m, water depths were converted to bed level elevations with respect to NAP.

We were able to map the banks of the South shore with the GPS and the rover by foot until a water depth of approximately 1.5 m.

The data from the two different sources (GPS and echo sounder) was put together, was interpolated and a mapped with QGIS.

A.3. Results

The result of the field survey is a merged topography and bathymetry map of the South shore of the Noorderplas. The map is shown in Figure A.3.

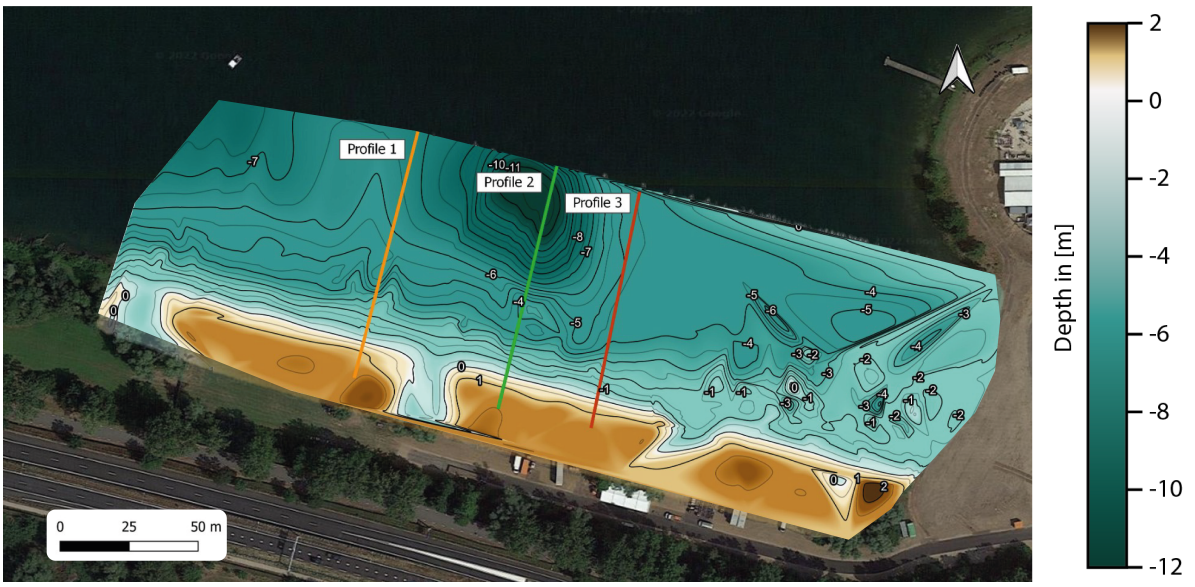

Figure A.3: Ground and lake bed level elevations South shore Noorderplas

From the map cross-shore profiles of the lake banks are extracted and shown in Figure A.4.

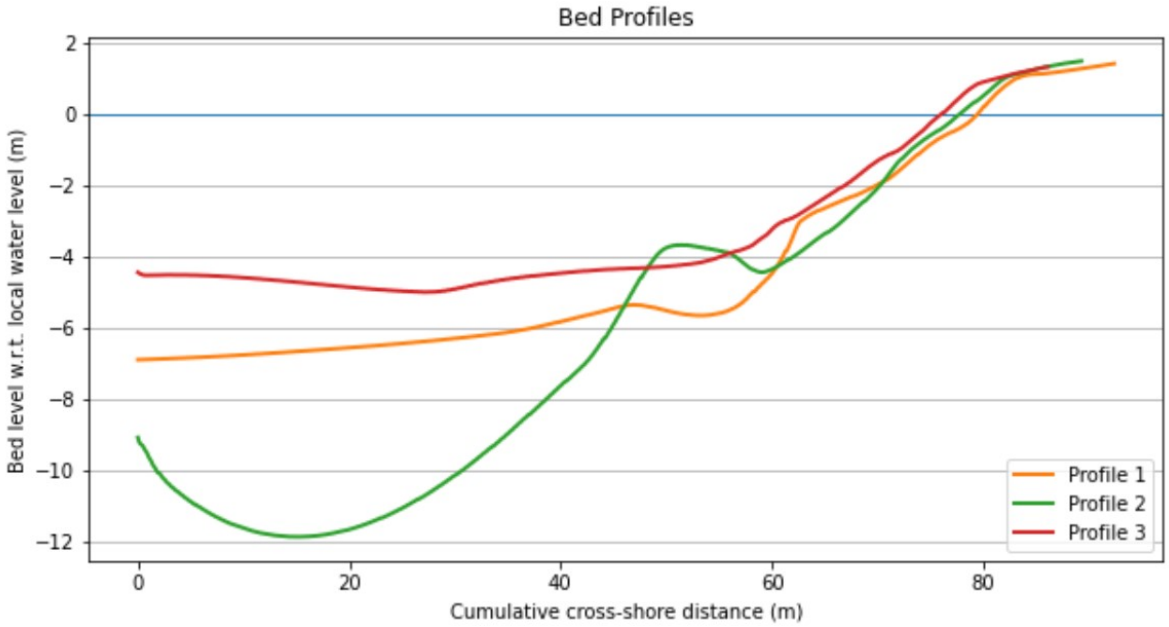

Figure A.4: Cross-shore profiles South shore Noorderplas.

B

DINOloket soil probes Noorderplas

The DINOloket has various soil probes available from the Noorderplas. In this section three soil profiles derived from soil probes from the Noorderplas are shown. Figure B.1 gives an overview of the locations of the soil probes. The probes are shown in Figure B.2, Figure B.3 and Figure B.4

Figure B.1: DINOloket - Noorderplas soil probe locations

Boormonsterprofiel

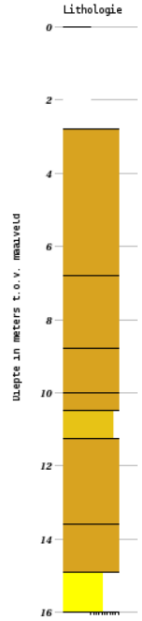

Identificatie :	B58D0358
Coördinaten :	195970 , 357470 (RD)
Maaiveld:	18.00 m t.o.v. NAP
Beschikbare informatie:	Digitale opnamegegevens
Beschrijfmethode:	Onbekend

Lithologie

- Zand fijne categorie
- Zand grove categorie
- Grind
- Niet benoemd

Figure B.2: Soil probe B58D0358

Boormonsterprofiel

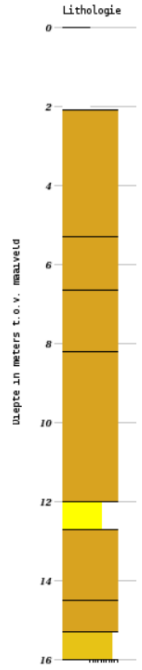

Identificatie :	B58D0359
Coördinaten :	195750 , 357550 (RD)
Maaiveld:	18.00 m t.o.v. NAP
Beschikbare informatie:	Digitale opnamegegevens
Beschrijfmethode:	Onbekend

Lithologie

- Zand fijne categorie
- Zand grove categorie
- Grind
- Niet benoemd

Figure B.3: Soil probe B58D0359

Boormonsterprofiel

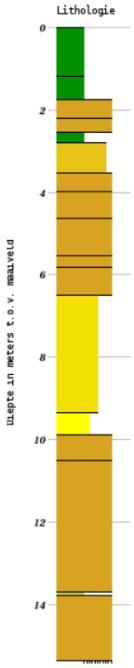

Identificatie :	B58D0046
Coördinaten :	195590 , 357070 (RD)
Maaiveld:	16.19 m t.o.v. NAP
Beschikbare informatie:	Digitale opnamegegevens
Beschrijfmethode:	Onbekend

Lithologie

- Leem
- Klei
- Zand fijne categorie
- Zand midden categorie
- Zand grove categorie
- Grind

Figure B.4: Soil probe B58D0046

C

Technical Drawings

The technical drawings of the wavepool that are provided by 24/7Waves are shown in Figure C.1 and Figure C.2. The drawings show a cross-section of the wavepool with the dimensions. These drawings are used as starting point for the design study.

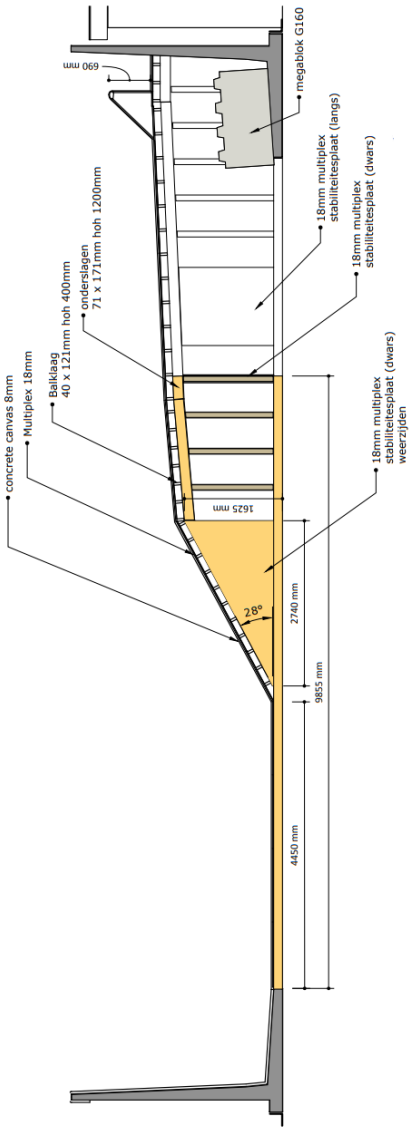

Figure C.1: Cross-section of the wavepool in the Binckhorst

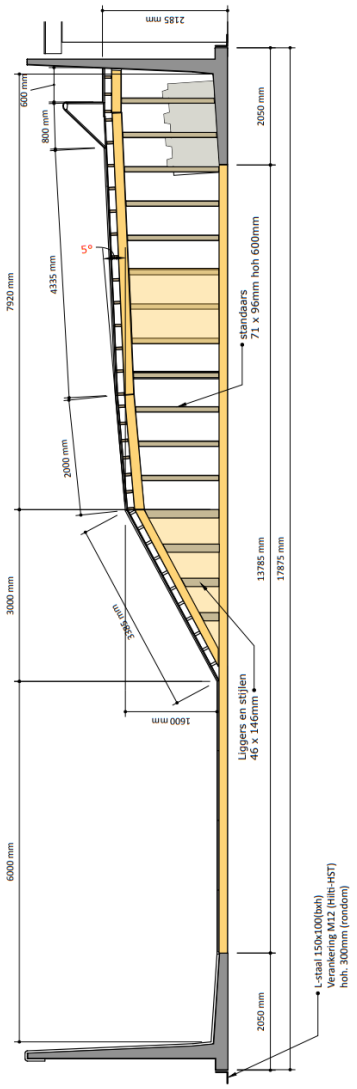

Figure C.2: Cross-section of the wavepool in the Binckhorst

D

Stability and erosion under wave loads

D.1. Wave transmission detached breakwaters

Parameters to which influence the wave transmission of a detached breakwater are: structural geometry, permeability, crest free-board, crest width, surface roughness, water depth, wave height and wave period. In an empirical study about the wave transmission at low-crested structures, d'Angremond et al., 1997 has defined the effectiveness of the detached breakwater with a transmission coefficient Kt. How much wave energy is transmitted over the breakwater depends on the dimensions and the characteristics of the breakwater.

$$K_t = \frac{W_{crest}}{H_i}^{-0.31} \cdot (1 - e^{-0.5\xi}) \cdot A_{dam} - 0.4 \cdot \frac{h_d}{H_i} \tag{D.1}$$

The effect of obliquely incident waves can be included by multiplying Equation D.1 with $(cos\beta)^{2/3}$. In which β represents the wave angle of incidence (van der Meer et al., 2005).

D.2. Stability of loose rock revetments

Bank revetments are loaded by primary and secondary waves. The main components that impact the banks are the return current, the stern wave and the secondary wave train. When determining the minimal rock size for the stability against ship waves a van der Meer or Hudson approach can be used. The damage level S and the impact frequency N should be accounted for. Typical values for very little damage are given by $S = 2$ and for very frequent wave attack $N = 7000$. It has been found that the stern wave is governing for stability (Schiereck, 2017). A Hudson's type of approach has resulted in the following design formula:

$$\frac{z_{max}}{\Delta \cdot d_{n50}} = 1.8cot(\alpha)^{0.33} \tag{D.2}$$

A van der Meer equation has been found for loose rock stability against the secondary wave train.

$$\frac{H}{\Delta \cdot d_{n50}} = 3.6\xi^{-0.5} \tag{D.3}$$

With:

- z_{max}: the stern wave height in m.
- Δ: the relative density given by $(\rho_{rock} - \rho_w)/\rho_w$.
- D_{n50}: the median nominal stone diameter in m.
- $cot\alpha$: the slope of the bank.
- ξ: the Iribarren parameter.

When wave transmission takes place at low crested structures, the median nominal stone diameter d_{n50} can be reduced with a certain factor. This factor was derived by van der Meer and holds for emerged breakwaters.

$$Reductiond_{n50} = \frac{1}{1.25 - 4.8\frac{R_c}{H}\sqrt{\frac{S_0}{2\pi}}} \tag{D.4}$$

For submerged breakwater the following relation holds:

$$\frac{H}{\Delta d_{n50}} = -7ln(\frac{h_c}{(2.1 + 0.1S)h}) \cdot s_p^{1/3} \tag{D.5}$$

With:

- R_c: the crest height relative to the water level in m.
- $s0_p$: the deep water wave steepness.
- h_c: the water depth at crest level in m.
- h: water depth in m.
- s_p: the wave steepness.

D.3. Stability of impervious protection layers

The main loads that an impervious layer on the detached breakwater would experience under ship waves are: uplift due to fluctuating wave pressure and direct wave impacts that exceed the materials. The layer can withstands these loads by sufficient layer thickness and stiff subsoil. These failure mechanisms are schematically shown in Figure D.1. Relations between loads and resistance have been derived empirically.

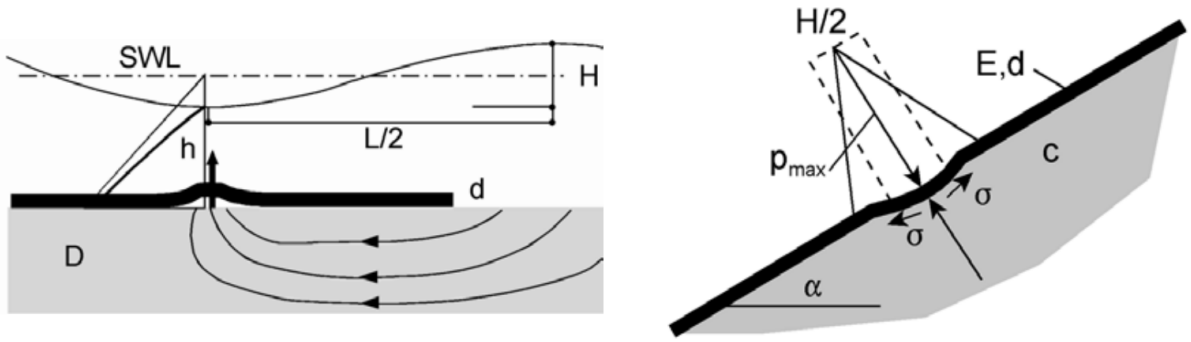

Figure D.1: Left: Uplift of the impervious layer. Right: Wave impact induced stresses (Schiereck, 2017)

Under fluctuating wave pressure, at the edge of the impervious layer, the layer can experiences an uplift force (Schiereck, 2017). Equilibrium of the impervious layer against uplift can be assessed with:

$$(\rho_m - \rho_w)gd > \rho_w g\frac{H}{2cosh(\frac{2\pi h}{L})} \tag{D.6}$$

With:

- ρ_m: the density of the material in kg/m3.
- ρ_w: the density of the water in kg/m3.
- g: the gravitation constant in m/s2.
- d: the layer thickness in m.

- H: the local wave height in m.
- h: the local depth in m.
- L: the local wave length in m.

The strength of impervious layer against failure can be assessed by comparing the wave impact induced stresses with the material properties:

$$\sigma = \frac{3p_{max}}{\beta^3 H d^2}[1 - \exp(\frac{-\beta H}{2})(\cos\frac{\beta H}{2} + \sin\frac{\beta H}{2})] \tag{D.7}$$

In which:

- σ: is the wave impact induced stresses in Pa.
- p_{max}: is the value to describe the wave impact. This values is given by $8\rho_w g H \cdot tan\alpha$.
- α the slope of the breakwater in degrees.
- H: the wave height in m.
- d: the layer thickness in m.

and:

$$with: \beta = \sqrt{\frac{2.65c}{Ed^3}} \;\&\; p_{max} = \rho_w g q H_s \tag{D.8}$$

In which:

- E: is the elasticity modulus of the material in Pa
- c: the stiffness of the subsoil in Pa/m

The failure stress of the layer depends on both the elasticity modulus and the stiffness of the subsoil. The relation is depicted in Figure D.2.

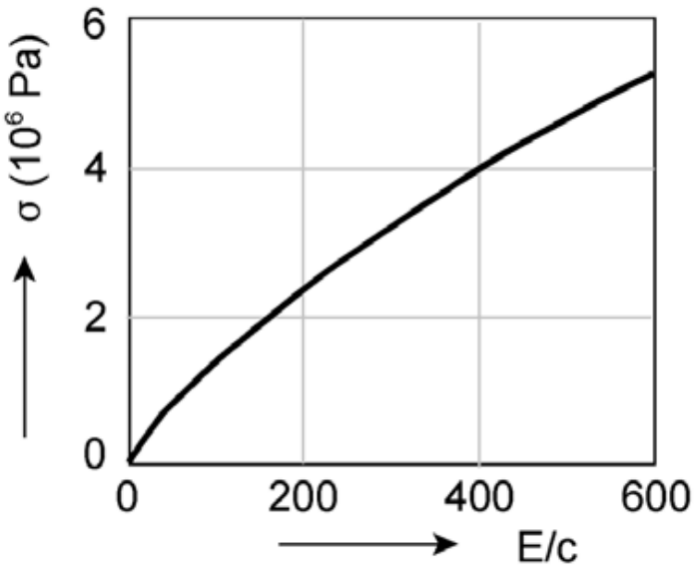

Figure D.2: Determine the failure stress (Schiereck, 2017)

It should be noted that this approach does not include the phenomena of failure due to long lasting wave attack causing fatigue.

E

Random-phase/amplitude model and linear wave theory

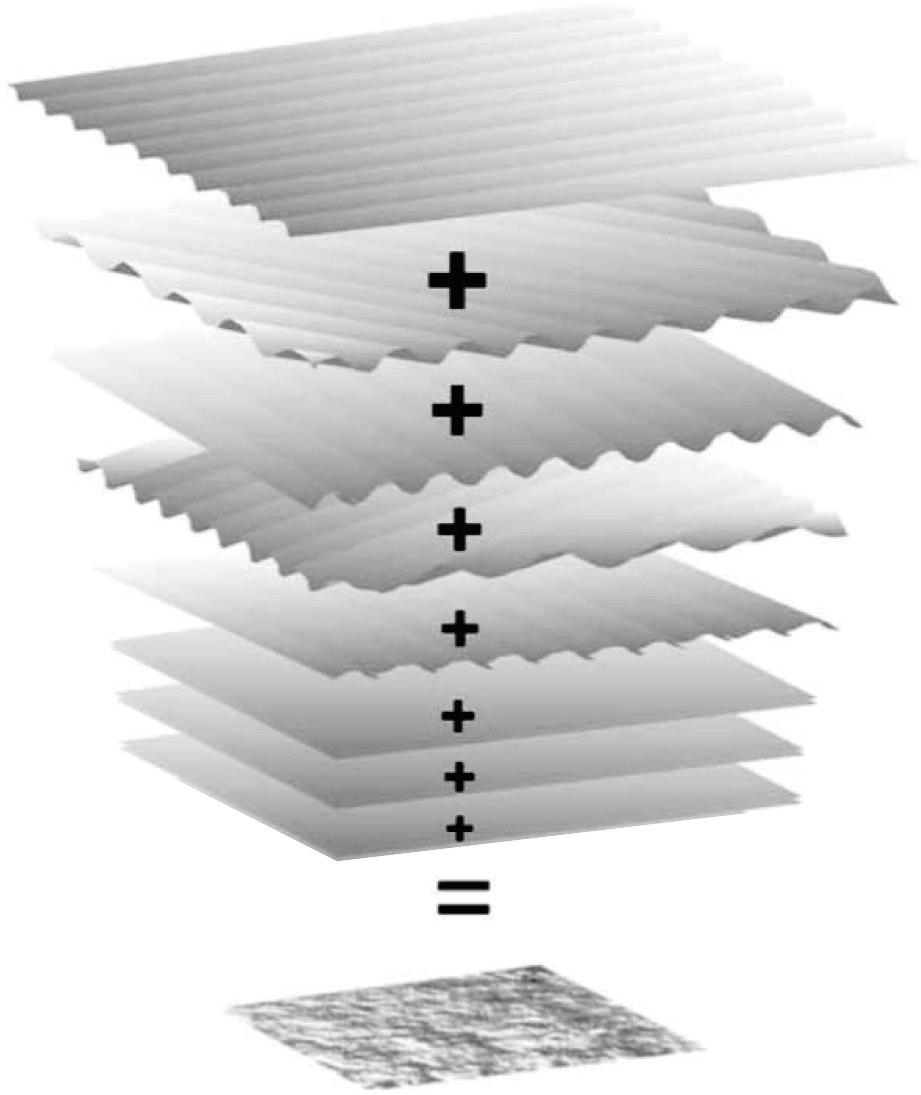

Figure E.1: Random-phase/amplitude model (Holthuijsen, 2010).

Parameter	Units	Shallow water	Transitional water depth	Deep water
wave profile	m	$\rightarrow$	$\eta = \frac{H}{2}\cos(kx - \omega t)$	$\leftarrow$
wave celerity	m/s	$c = \frac{L}{T} = \frac{\omega}{k} = \sqrt{gh}$	$c = \frac{L}{T} = \frac{\omega}{k} = \sqrt{\frac{g}{k}\tanh kh} = \frac{gT}{2\pi}\tanh kh$	$c = c_0 = \frac{L}{T} = \frac{gT}{2\pi} = \frac{g}{\omega}(\simeq 1.56T)$
wave group celerity	m/s	$c_g = c = \sqrt{gh}$	$c_g = nc = \frac{1}{2}\left[1 + \frac{2kh}{\sinh 2kh}\right]c$	$c_{g0} = \frac{1}{2}c_0 = \frac{gT}{4\pi}$
wavelength	m	$L = cT = \sqrt{gh}T$	$L = cT = \frac{gT^2}{2\pi}\tanh kh$	$L = L_0 = c_0T = \frac{gT^2}{2\pi}(\simeq 1.56T^2)$
wave particle velocity horizontal	m/s	$u = \frac{\omega H}{2kh}\cos(kx - \omega t)$	$u = \frac{\omega H}{2}\frac{\cosh kz}{\sinh kh}\cos(kx - \omega t)$	$u = \frac{\omega H_0}{2}\exp k_0(z_0 - h)\cos(k_0x - \omega t)$
... vertical	m/s	$w = \frac{\omega Hz}{2h}\sin(kx - \omega t)$	$w = \frac{\omega H}{2}\frac{\sinh kz}{\sinh kh}\sin(kx - \omega t)$	$w = \frac{\omega H_0}{2}\exp k_0(z - h)\sin(k_0x - \omega t)$
wave particle acceleration horizontal	m/s^2	$a_x = \frac{\omega^2 H}{2kh}\sin(kx - \omega t)$	$a_x = \frac{\omega^2 H}{2}\frac{\cosh kz}{\sinh kh}\sin(kx - \omega t)$	$a_x = \frac{\omega^2 H_0}{2}\exp k_0(z - h)\sin(k_0x - \omega t)$
... vertical	m/s^2	$a_z = \frac{-\omega^2 Hz}{2h}\cos(kx - \omega t)$	$a_z = \frac{-\omega^2 H}{2}\frac{\sinh kz}{\sinh kh}\cos(kx - \omega t)$	$a_z = \frac{-\omega^2 H_0}{2}\exp k_0(z - h)\cos(k_0x - \omega t)$
wave particle displacement horizontal	m	$\xi = \frac{-H}{2kh}\sin(kx - \omega t)$	$\xi = \frac{-H}{2}\frac{\cosh kz}{\sinh kh}\sin(kx - \omega t)$	$\xi = \frac{-H_0}{2}\exp k_0(z - h)\sin(k_0x - \omega t)$
... vertical	m	$\xi = \frac{Hz}{2h}\cos(kx - \omega t)$	$\xi = \frac{H}{2}\frac{\sinh kz}{\sinh kh}\cos(kx - \omega t)$	$\xi = \frac{H_0}{2}\exp k_0(z - h)\cos(k_0x - \omega t)$
subsurface pressure	N/m^2	$p = \rho g(h - z) + \frac{\rho gH}{2}\cos(kx - \omega t)$	$p = \rho g(h - z) + \frac{\rho gH}{2}\frac{\cosh kz}{\cosh kh}\cos(kx - \omega t)$	$p = \rho g(h - z) + \frac{\rho gH_0}{2}\exp k_0(z - h)\cos(kx - \omega t)$
wave energy per wavelength per unit crest length	J/m	$E_t = {}^1/_8\rho gH^2L$	$E_t = {}^1/_8\rho gH^2L$	$E_0 = {}^1/_8\rho gH_0^2L_0$
specific wave energy	J/m^2	$E_t = {}^1/_8\rho gH^2$	$E_t = {}^1/_8\rho gH^2$	$E_0 = {}^1/_8\rho gH_0^2$
wave power	J/ms	$U = Ec_g = Enc = Ec$	$U = Ec_g = Enc$	$U_0 = E_0n_0c_0 = {}^1/_2E_0c_0$

Figure E.2: Expressions for wave characteristics according to the linear wave theory (Holthuijsen, 2010).